REPUBLIC OF TÜRKİYE
KARADENIZ TECHNICAL UNIVERSITY
GRADUATE SCHOOL OF HEALTH SCIENCES

DEPARTMENT OF MEDICAL BIOCHEMISTRY

INVESTIGATION OF THE EFFECT OF L-THEANINE ON GLUCOSE AND LIPID METABOLISM IN RATS TREATED WITH DOXORUBICIN

Entesar Ali Ahmed AMER

MASTER'S THESIS

Prof. Dr. Birgül KURAL

TRABZON-2025

DECLARATION

I declare that this thesis was accomplished and written in accordance with the standards of Karadeniz Technical University Graduate School of Health Sciences Thesis Preparation and Writing Guide. The present thesis is original scientific research carried out by committing to academic and ethical rules. I confirm that I have cited the sources of any information or comments that were not obtained by the present study in the list of references, and I have not acted in violation of patents and copyrights during the study and writing of the thesis.

14/08/2025

Entesar Ali Ahmed AMER

Dedication

I humbly dedicate this work to my beloved family, my great parents, Fatma and Ali AMER, and my elder brother, Ahmed, for giving me everything they had to get here. I also extend my gratitude to my relatives and friends who supported me. Also, I would like to express my heartfelt gratitude to my dear friend Kawther ALEDRESI, who accompanied me on my journey.

ACKNOWLEDGMENTS

I owe a deep debt of gratitude to my university, Karadeniz Technical University, for giving me an opportunity to perform a master's degree and research.

I am extremely grateful to my advisor, Prof. Dr. Birgül KURAL, for her support, invaluable guidance, unwavering patience, and genuine care throughout the entirety of this project have meant a great deal to me. Your motivation and enthusiasm supported me at every stage, and their impact will remain with me always.

My appreciation goes to the members of the Medical Biochemistry Department, Prof. Dr. Asım ÖREM, Prof. Dr. Süleyman Caner KARAHAN, Prof. Dr. Yüksel ALİYAZICIOĞLU, Prof. Dr. Ahmet ALVER, Prof. Dr. Ahmet MENTEŞE, Prof. Dr. Selim DEMİR, Assoc. Prof. Fulya BALABAN YÜCESAN and Assist. Prof. Dr. Hüseyin YAMAN for the profound impact you have had on my academic journey

I would like to extend my appreciation to Res. Asst. Dr. Sevil KÖR for her valuable support in both laboratory procedures and statistical analyses. My sincere thanks go to the teaching staff, whose contributions significantly enriched my academic experience. I extend my gratitude to Assoc. Prof. Serap ÖZER YAMAN from the Department of Medical Biochemistry, Faculty of Medicine, University of Health Sciences.

I am sincerely thankful to Prof. Dr. Sedat BOSTAN, Director of the Graduate School of Health Sciences, along with Prof. Dr. Selim DEMİR and Assoc. Prof. Aysel ÖZSABAN, and to all administrative team.

My sincere thanks also go to all my family members, my best friends, and childhood and study friends for their continuous support and encouragement.

Entesar Ali Ahmed AMER

TABLE of CONTENTS

LIST of TABLES

LIST of FIGURES

LIST of ABBREVIATIONS, SYMBOLS and FORMULA

Abbreviations

4-AAP	4-Aminoantipyrine
AKT	Protein Kinase B
ALT	Alanine Transaminase
AMPK	AMP-Activated Protein Kinase
AST	Aspartate Aminotransferase
ATP	Adenosine Triphosphate
CD36	Cluster of Differentiation 36
CHE	Cholesterol Esterase
CHO	Cholesterol Oxidase
CLD	Chronic Liver Disease
DXN	Doxorubicin
ELISA	Enzyme-Linked Immunosorbent Assay
ER	Endoplasmic Reticulum
FAT	Fatty Acid Translocase
FFA	Free Fatty Acids
G-1-P	Glycerol-1-Phosphate
G6P	Glucose-6-Phosphate
G6P-DH	Glucose-6-Phosphate Dehydrogenase
GCL	Glutamate Cysteine Ligase
GLUT-4	Glucose Transporter-4
GPx4	Glutathione Peroxidase 4
GR	Glutathione Reductase
GSH	Glutathione
GSS	GSH Synthetase
GSSG	Glutathione Disulfide
Hcy	Homocysteine
HDL-C	High Density Lipoprotein-Cholesterol
HK	Enzymatic Hexokinase
HSL	Hormone-Sensitive Lipase
IREs	Iron-Response Elements

IRP	Iron Regulatory Proteins
ISM1	Isthmin-1
LDH	Lactate Dehydrogenase
LDL-C	Low-Density Lipoprotein-Cholesterol
LT	L-theanine
MDA	Malondialdehyde
NAD⁺	Nicotinamide Adenine Dinucleotide
NADH	Nicotinamide Adenine Dinucleotide Hydride
NF-κB	Nuclear Factor Kappa-Light-Chain-Enhancer of Activated B Cells
Nrf2	Nuclear Factor Erythroid 2–Related Factor 2
PBS	Phosphate-Buffered Saline
PLOOHs	Phospholipid Hydroperoxides
POD	Peroxidase
PPARγ	Peroxisome Proliferator-Activated Receptor Gamma
RNS	Reactive Nitrogen Species
ROS	Reactive Oxygen Species
SAH	S-adenosylhomocysteine
SREBP-1c	Sterol Regulatory Element Binding Protein-1
T2DM	Type 2 Diabetes Mellitus
TBA	Thiobarbituric Acid
TC	Total Cholesterol
TG	Triglyceride
t-GPx4	Tissue Glutathione Peroxidase 4
t-GSH	Tissue Glutathione
t-GSSG	Tissue Glutathione Disulfide
t-ISM1	Tissue Isthmin-1
t-MDA	Tissue - Malondialdehyde
TNF-α	Tumor Necrosis Factor-Alpha
TPTZ	2,4,6-Tri-(2-Pyridyl)-5-Triazine
t-TC	Tissue Total Cholesterol
t-TG	Tissue Triglyceride
t-TNF-α	Tissue Tumor Necrosis Factor-Alpha
t-ZAG	Tissue Zinc-α-Glycoprotein

| VLDL | Very Low-Density Lipoprotein |
| ZAG | Zinc-α-Glycoprotein |

Symbols

&	And
α	Alpha
β	Beta
γ	Gamma
κ	Kappa

Formula

$C_{27}H_{29}NO_{11}$	Doxorubicin
$C_7H_{14}N_2O_3$	L- Theanine
Fe	Iron
H_2O	Water
H_2O_2	Hydrogen Peroxide
H_3PO_4	Phosphoric acid
KCl	Potassium Chloride
NaCl	Sodium Chloride
O_2	Oxygen
O_2^-	Superoxide
$OH^{\cdot}$	Hydroxyl Radicals

ABSTRACT

Investigation of the Effect of L-Theanine on Glucose and Lipid Metabolism in Rats Treated with Doxorubicin

Doxorubicin (DXN) is a powerful chemotherapeutic agent, commonly used to treat solid tumors and hematologic malignancies. It has side effects on glucose and lipid metabolism. It is known to induce oxidative stress and inflammation. L-theanine (LT) is a non-protein amino acid found in tea. It has multiple biological benefits, including regulating glucose and lipid metabolism and exhibiting anti-inflammatory activity. Our study aimed to evaluate the effectiveness of LT on the parameters involved in glucose and lipid metabolism in Wistar rats treated with DXN. This study involved 28 rats with four groups (n=7/group): Control, DXN, DXN+LT200, and DXN+LT400. DXNs were applied at 6 mg/kg/dose (3 doses on the 4th, 11th, and 18th days), and 200 and 400 mg/kg/day of LT treatments were given by oral gavage for 21 days. The levels of insulin, isthmin-1 (ISM1), zinc-α-glycoprotein (ZAG), free fatty acids (FFA), glutathione peroxidase 4 (GPx4), tumor necrosis factor-alpha (TNF-α), and reduced and oxidized glutathione (GSH and GSSG, respectively) were determined in serum and/or liver tissue by using commercial kits, and serum iron (Fe) and liver malondialdehyde (MDA) by colorimetric methods. While DXN administration increased cholesterol, triglyceride, ISM1, and ZAG levels in the serum and liver, LT treatment, particularly at 400 mg/kg/day, decreased the levels of these parameters. DXN also increased serum iron levels and decreased insulin levels. LT treatment reversed these effects. In conclusion, the presence study suggested that insulin, ISM1, and ZAG proteins may play roles in DXN's effects on glucose and lipid metabolism. LT treatment had the potential to alter these effects. Further studies are needed to elucidate the effects of DXN and LT treatments on parameters involved in metabolism regulation.

Keywords: Doxorubicin, Insulin, Isthmin-1, Zinc-α-glycoprotein

ÖZET

Doksorubisin Uygulanan Sıçanlarda Glukoz ve Lipid Metabolizmasına L-Teaninin Etkisinin Araştırılması

Doksorubisin (DXN), katı tümörlerin ve hematolojik malignitelerin tedavisinde yaygın olarak kullanılan güçlü bir kemoterapötik ajandır. Glukoz ve lipit metabolizması üzerinde yan etkileri vardır. Oksidatif stres ve inflamasyonu tetiklediği bilinmektedir. L-teanin (LT), çayda bulunan protein yapısına dahil olmayan bir amino asittir. Glukoz ve lipit metabolizmasını düzenleme ve antiinflamatuar etki gösterme gibi birçok biyolojik faydası vardır. Çalışmamız, DXN ile tedavi edilen Wistar sıçanlarında glukoz ve lipit metabolizması ile ilgili parametreler üzerinde LT'nin etkinliğini değerlendirmek amacıyla yapılmıştır. Bu çalışmaya dört grupta (n=7/grup) 28 sıçan dahil edildi: Kontrol, DXN, DXN+LT200 ve DXN+LT400. DXN'lar 6 mg/kg/doz (4., 11. ve 18. günlerde 3 doz) olarak uygulandı ve 200 ve 400 mg/kg/gün LT tedavileri 21 gün boyunca oral gavaj yoluyla verildi. İnsülin, istmin-1 (ISM1), çinko-α-glikoprotein (ZAG), serbest yağ asitleri (FFA), glutatyon peroksidaz 4 (GPx4), tümör nekroz faktörü-alfa (TNF-α) ve indirgenmiş ve okside glutatyon (sırasıyla GSH ve GSSG) düzeyleri, serum ve/veya karaciğer dokusunda ticari kitler kullanılarak, serum demir (Fe) ve karaciğer malondialdehit (MDA) düzeyleri ise kolorimetrik yöntemlerle belirlendi. DXN uygulaması serum ve karaciğerde kolesterol, trigliserit, ISM1 ve ZAG düzeylerini artırırken, LT tedavisi, özellikle 400 mg/kg/gün dozunda, bu parametrelerin düzeylerini düşürdü. DXN, ayrıca, serum demir düzeylerini artırdı ve insülin düzeylerini düşürdü. LT tedavisi bu etkileri tersine çevirdi. Sonuç olarak, bu çalışma insülin, ISM1 ve ZAG proteinlerinin DXN'nin glukoz ve lipit metabolizması üzerindeki etkilerinde rol oynayabileceğini gösterdi. LT tedavisi bu etkileri değiştirebilme potansiyeline sahipti. DXN ve LT tedavilerinin metabolizmanın düzenlemesinde rol alan parametreler üzerindeki etkilerini aydınlatmak için daha fazla çalışma ihtiyaç vardır.

Anahtar Sözcükler: Çinko-α-glikoprotein, Doksorubisin, İnsülin, İstmin-1

1. INTRODUCTION and AIM

Doxorubicin (DXN) is an anthracycline chemotherapeutic agent indicated for some solid tumors (gastrointestinal, ovarian, breast, brain, etc.) and hematological malignancies (lymphoma and leukemia) (1). This drug causes intercalation between the nitrogenous bases of DNA and impedes the process of macromolecule biosynthesis. On the other hand, DXN exhibits harmful effects in many healthy tissues, including white adipose tissue, liver, skeletal, and cardiac muscle (2).

The predominant mechanism through which DXN-induced liver damage occurs is via oxidative stress and apoptotic pathways (3). Inactivation of iron-regulating proteins has a role in the increase of oxidative stress by DXN. Because iron generates reactive oxygen species (ROS) via the Fenton reaction, this triggers lipid peroxidation (4). Liver damage develops when DXN increases oxidative stress. Hepatic enzymes, including alanine transaminase (ALT) and aspartate aminotransferase (AST), increase in the blood with increased cellular permeability; hepatic damage leads to a decrease in total protein and albumin levels (5).

DXN has been demonstrated to influence body weight, the levels of blood glucose and lipids, making symptoms similar to those of type 2 diabetes (T2DM). It also suppresses peroxisome proliferator-activated receptor gamma (PPARγ), which controls the expression of glucose and fatty acid transporters. It causes hyperglycemia and hyperlipidemia by increasing blood glucose and inhibiting lipid clearance, leading to glucotoxicity, lipotoxicity, insulin resistance and inflammation (6).

ISM1 is an adipokine that is highly expressed in various tissues (7, 8). It has a crucial role in glucose and lipid metabolism through its insulin-like properties (9). ISM1 has been recognized for its role in modulating glucose uptake within adipose tissue and suppressing hepatic lipogenesis (8). In an experimental study, an increase in ISM1 levels following DXN treatment was reported, which may be linked to ISM1's role in inducing apoptosis (10).

ZAG is a vital adipokine that has a significant role as a lipid-mobilizing factor in adipose tissue. It helps maintain a healthy body weight via promoting lipolysis in adipocytes (11, 12). It is expressed in multiple tissues and then released into the body fluid. However, liver and adipose tissues are the main sites for ZAG synthesis (11, 13). In subcutaneous adipose tissue, a positive correlation exists between insulin sensitivity and the expression of

1

glucose transporter-4 (GLUT-4) mRNA and ZAG. In contrast, a decrease in ZAG affects glucose metabolism (13).

LT is an essential non-protein amino acid found in tea. Various physiological functions of LT, including antioxidant, anti-inflammatory, hepatoprotective, and immune-modulating properties, have been identified (14, 15). LT is metabolized into glutamate in liver, and glutamate serves as the precursor to GSH, a powerful antioxidant. It has been suggested that LT may regulate glucose, lipid, and protein metabolism (16).

In the present study, we aimed to evaluate the effectiveness of LT on the parameters that contribute to regulating glucose and lipid metabolism in rats treated with DXN.

2. LITERATURE REVIEW

2.1. Doxorubicin

2.1.1. General Properties of Doxorubicin

Doxorubicin (DXN), also known as adriamycin (chemical formula: $C_{27}H_{29}NO_{11}$). It is an antineoplastic agent considered one of the antibiotic drugs, derived from the *Streptomyces peucetius* bacterium. Since the 1960s, it has been widely used in chemotherapy, mainly in treating solid tumors. It is known to be effective against some cancers, including hematologic malignancies, sarcomas, and carcinomas of the breast, lung, ovaries, thyroid, and bladder. DXN can be used either alone or combined with other anticancer agents as a first-line therapy for bladder (1, 3, 17). DXN is usually administered intravenously. DXN may go through a catheter in the chest and remain in place throughout the treatment. It can be applied peripherally by inserting a central catheter. In case the patient does not have a central line, DXN might be administered through a cannula in the patient's arm. This cannula should be renewed each time a DXN treatment is performed (18).
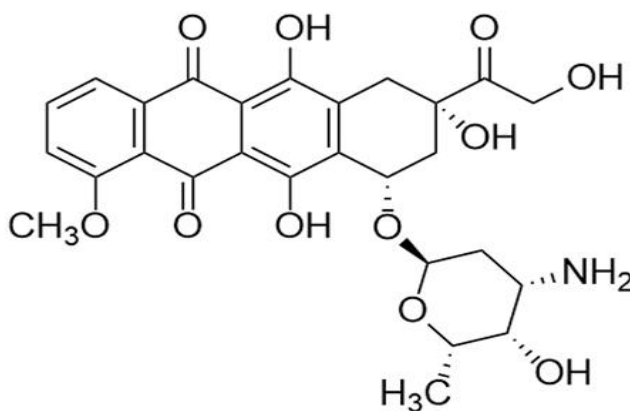
Figure 1. Doxorubicin chemical structure (from Mattioli, 3)

DXN exhibits its anticancer activity through multiple mechanisms, many of which depend on drug binding to DNA, thereby affecting DNA structure and ultimately leading to cell death (19). Anthracyclines are mostly planar, aromatic molecules that can intercalate with DNA by inserting between base pairs, thereby separating adjacent base pairs and being anchored to the DNA minor groove by the sugar moiety (2, 20). DXN intercalates with DNA through hydrogen bonding with guanine, which disrupts the DNA replication and

transcription processes. This leads to an untwisted DNA molecule, which causes positive supercoiling of the DNA helix and therefore destabilizes nucleosomes (3, 19). Anthracyclines, in general, can form adducts with DNA by covalent and hydrogen bonds with the two DNA strands. This results in disturbance of normal DNA function, blocking replication and transcription. In contrast to intercalation, which is reversible, DNA adduct formation is more permanent, leading to long-lasting DNA damage and cell death (2).

2.1.2. Doxorubicin Side Effects

Besides its chemotherapeutic activity, the usage of DXN has been limited due to its side effects. It harms multiple organs, causing toxicity such as cardiotoxicity, hepatotoxicity, and nephrotoxicity. It has been reported that DXN induced hepatotoxicity at acute and sub-acute doses. Since the liver is the main organ that is responsible for detoxifying and breaking down the drugs, that makes the liver highly exposed to the toxic effects of DXN (1).

2.1.2.1. Oxidative Stress and Inflammation

Oxidative stress is defined as an imbalance between reactive oxygen and nitrogen species (ROS and RNS, respectively) and the body's antioxidant defense system. When reactive species levels become exaggerated, that will lead to damaging cells' proteins and lipids, resulting in cellular dysfunction (21). DXN is known to induce oxidative stress and inflammation, which lead to significant toxicities. DXN metabolism in the liver causes the generation of ROS, including superoxide (O_2^-), hydrogen peroxide (H_2O_2), and hydroxyl radicals ($OH^{\bullet}$). These ROS change the redox balance; moreover, hepatocytes can't maintain a stable oxidative environment. It has been mentioned that DXN administration disrupts hepatocyte cell cycle progression. Hepatocytes are the main functional cells of the liver; they undergo a regulated cell cycle to maintain liver functions. DXN disruption for hepatocytes leads to cell cycle inhibition, reduces the liver's repair ability, and causes tissue damage (3, 22).

DXN can disrupt iron homeostasis through the inactivation of iron regulatory proteins 1 and 2 (IRP1 and IRP2). Therefore, IRPs bind to iron-response elements (IREs), which are specific sequences in mRNA (4). While iron levels are low, IRPs are still active and can bind to IREs, resulting in the control of ferritin synthesis gene expression. When DXN inactivates IRPs, it causes changes in ferritin protein synthesis. When IRPs are active, ferritin mRNA translation is prevented. While the inactivation of IRPs elevates ferritin production, thereby increasing labile iron. Simultaneously, DXN increases transferrin

4

receptor, a receptor responsible for transporting iron into the cell. That will increase the amount of free intracellular iron, leading to ferroptosis (4). DXN can disrupt the cell oxidation-reduction balance, and this is done by triggering iron-dependent lipid peroxidation (2). Ferroptosis is an iron-dependent form of oxidative cell death characterized by diminished GSH. As DXN disrupts the redox balance, it leads to not only lipid peroxidation but also results in adenosine triphosphate (ATP) depletion and DNA damage. This causes oxidative stress that damages the cell membrane (2, 23).

GSH is a non-protein tripeptide and a major modulator of redox processes, serving as a cofactor for several antioxidant enzymes such as glutathione reductase (GR), GPx, and glutathione S-transferase (GST) (24). GSH is synthesized in the cytosol by glutamate cysteine ligase (GCL) and GSH synthetase (GSS) action. Transportation of GSH to the endoplasmic reticulum (ER), nucleus, and mitochondria occurs by multidrug-associated resistance protein and porins. When oxidative stress happens, GSH is converted to GSSG. GR regenerates the GSH pool. When the body is exposed to various oxidants, xenobiotics, and antioxidants, this stimulates GSS through the nuclear factor erythroid 2-related factor 2 (Nrf2) transcription factor, leading to upregulation of GCL and GSS. The antioxidant system in the liver, including GSH, plays a vital role in alleviating this damage. GSH helps regenerate vitamin C and E by becoming oxidized when reacting with ROS and lipid peroxides (25). Meanwhile, GSH depletion triggers toxicity. Jointly, elevating the level of lipid peroxidation product, MDA, is an additional indicator for oxidative stress-related to liver damage (26). The GPx family of enzymes is considered the largest group containing selenoproteins. There are eight isozymes of GPxs, which are different in terms of where they are located and how specific they are to phospholipid peroxides, cholesterol peroxides, and other substrates. GPx4 is one of the five isozyme members that contain selenium in the catalytic site. It is known to be a key regulator of non-apoptotic cell death, known as ferroptosis (27). Therefore, the generation of highly reactive hydroxyl radicals leads to lipid peroxidation and subsequent cell damage (28). GPx4 is recognized as a key antioxidant enzyme responsible for neutralizing lipid peroxides (28). Moreover, GPx4 reduces phospholipid hydroperoxides (PLOOHs) to non-toxic lipid alcohols, thereby maintaining cellular redox balance and preventing ferroptotic cell death. Although iron overload and excessive amounts of PLOOHs lead to GPx4 inhibition, which worsens the oxidative damage (28).

Reactive species activate the signaling pathway, stimulating an inflammatory response. Molecules like TNF-α are released. This molecule triggers the production of other inflammatory molecules. Tumor necrosis factor alpha (TNF-α) is a pro-inflammatory cytokine. It has been reported as a major regulator of inflammatory responses. It is recognized as playing a role in the pathogenesis of some inflammatory and autoimmune diseases (28). TNF-α also stimulates the regulation of nuclear factor kappa-light-chain-enhancer of activated B cells (NF-κB). Then, NF-κB stimulates the transcription of pro-inflammatory cytokines and chemokines. Therefore, the inflammatory response may be amplified. The release of additional inflammatory molecules creates a positive feedback loop, resulting in increased inflammation (29). An increase in TNF-α circulating levels can be an indicator of cancer progression and a signal for lower survival rates. Elevated TNF-α levels correlate with insulin resistance, affecting insulin receptor signaling in muscle cells and adipocytes (30).

2.1.2.2. The Effect of Doxorubicin on Metabolism

DXN's effect on lipid and glucose metabolism has been examined through multiple studies, which have disclosed important disruptions in metabolic pathways. DXN affects glucose metabolism and can induce hyperglycemia and insulin resistance. It disturbs normal glucose utilization in multiple tissues, especially skeletal muscle and heart. Additionally, it can also mimic T2DM. According to the studies, DXN treatment causes high blood sugar levels (hyperglycemia) and reduces insulin sensitivity (31). This occurs due to the inhibition of AMP-activated protein kinase (AMPK), which is a pivotal regulator of glucose uptake and energy balance. Some studies mentioned that DXN affects adipose tissue metabolism, which is similar to how T2DM interrupts fat utilization in skeletal muscles. Treatment with DXN causes atrophy (muscle mass wasting), weight loss, and anorexia. This muscle-thinning condition results in a significant reduction in GLUT-4 protein and mRNA expression in skeletal muscle. GLUT-4 is an essential glucose transporter that helps muscle cells absorb glucose from the bloodstream. DXN treatment causes a reduction in insulin sensitivity. Insulin resistance appears when the proteins involved in the signaling cascade are suppressed (31). Because these proteins are essential for GLUT-4 translocation, a reduction in their activity inhibits skeletal muscle cells from effectively absorbing glucose (31).

PPAR-γ regulates the initiation of adipogenesis, transforming pre-adipocytes into mature adipocytes. Mature adipocytes are known to express fatty acid translocase/cluster of differentiation 36 (FAT/CD36) for fatty acid uptake and GLUT-4 for glucose uptake. Fatty acids are typically stored as triglycerides, while glucose plays a crucial role in supporting lipid storage and maintaining energy balance. DXN inhibits PPAR-γ, resulting in a reduction in adipogenesis and impairment of adipocyte maturation. This DXN-induced impairment leads to diminished mature adipocytes and reduces the tissue's capacity to store lipids sufficiently. In parallel, DXN downregulates FAT/CD36 and GLUT-4, which decreases glucose and fatty acids uptake. The accumulation of glucose and fatty acids can lead to glucotoxicity and lipotoxicity (6). Many studies have reported that DXN administration increases triglyceride (TG), very low-, low-, and high-density lipoprotein cholesterol (VLDL-C, LDL-C, and HDL-C, respectively) (32, 33).

2.1.2.3. Insulin Resistance

Insulin, a hormone, is produced by the β cells of the islets of Langerhans, which are located in the pancreas. These islets are approximately 1-2% of the total cells in the pancreas. It has a crucial anabolic effect on multiple tissues, including glucose metabolism, which induces glycogen synthesis and storage. It also induces free fatty acid (FFA) synthesis, TG storage, and protein synthesis. Insulin consists of 52 amino acids, forming two polypeptide chains, A and B, which are linked by two disulfide bonds. Moreover, it has an intramolecular disulfide bond between the amino acids in chain A. Insulin is biosynthesized in the membrane of rough ER in β-cells as a pre-proinsulin. Then, it is transferred to the lumen of the rough endoplasmic reticulum cisternae and converted to Proinsulin. Small vesicles that contain proinsulin are detached from the ER to fuse with the Golgi apparatus cisternae. Pancreatic β cells are glucose-sensing cells; when blood sugar increases after meals, they stimulate insulin secretion (34, 35).

Insulin resistance is a condition in which tissue decreases its ability to respond to the elevated insulin concentration in the blood (35). DXN leads to hyperglycemia and hyperlipidemia, which are caused by the inhibition of PPARγ (6, 31). A study showed that DXN decreases the expression of insulin receptor substrate-1, GLUT-4, and AMPK, which may induce insulin resistance (36).

2.2. Adipokines

Adipose tissue is not merely an energy reservoir; it is considered an endocrine organ with the ability to influence systemic homeostasis through the release of various adipokines. Adipokines are bioactive signaling molecules secreted predominantly by adipose tissue, functioning as metabolic regulators, mediators of inflammation, and endocrine signaling molecules (37, 38). Dysregulation of adipokines may contribute to obesity-related disorders, including T2DM, cardiovascular disease, and nonalcoholic fatty liver disease (37). Among emerging adipokines, ZAG and ISM1 have garnered attention for their lipolytic properties, which suppress hepatic lipogenesis and thereby ameliorate hyperglycemia and lipid accumulation in metabolic disease models (12, 39).

2.2.1. Isthmin-1

ISM1 is a novel adipokine first explored by Pera et al. (7) in the isthmus of Xenopus laevis throughout the brain's early development. It's highly expressed in multiple tissues, including thyroid, placenta, prostate, adipose tissue, lung, brain, and liver (8, 40). It plays a pivotal role in protein, glucose, and lipid metabolism via its insulin-like properties (9, 41). ISM1 is found in both brown and white adipose tissue; however, it is higher in brown adipose tissue, suggesting its role in energy regulation (39). Among the ISM1 functions, its importance has been highlighted in the regulation of glucose absorption in adipose tissue and the reduction of hepatic lipogenesis (8). Jiang et al. (39) have reported that ISM1 induces GLUT-4 translocation from the cytoplasm to the plasma membrane. Moreover, it stimulates glucose uptake via the phosphatidylinositol 3–kinase-protein kinase B (AKT)pathway. Notably, ISM1 and insulin share similarities in their effects on glucose utilization; however, they don't act on the same receptors (8, 39). Simultaneously, inhibiting hepatic lipogenesis (42). A significant reduction in ISM1 levels has been confirmed in T2DM subjects when compared to healthy subjects. ISM1 is considered an independent protective factor for the development of type 2 diabetes mellitus (T2DM) (8). As has been previously indicated, the dose of ISM1 has a significant impact on its ability to inhibit the insulin-induced expression of the pro-lipid synthesis factor sterol regulatory element binding protein-1c (SREBP-1c) and its target genes, acetyl-CoA carboxylase (ACC), fatty acid synthase, and LDL receptor. Additionally, ISM1 has been observed to weaken the insulin-induced lipogenesis (39). Accordingly, ISM1 can be used in the treatment of diseases associated with dysregulated glucolipid metabolism, such as T2DM (42). In the liver, ISM1 inhibits *de novo* lipogenesis;

simultaneously, in both the liver and muscles, it enhances protein synthesis via the AKT-mammalian target of rapamycin-S6 pathway. Therapeutic studies have shown that supplying mice with recombinant Ism1 protein improves glucose tolerance and reduces signs of fatty liver disease (hepatic steatosis) in obese and diabetic mouse models, indicating that ISM1 acts as a dual-function hormone (39). It is involved in controlling angiogenesis, which is crucial during both normal physiological processes (e.g., wound healing) and pathological conditions (e.g., cancer). ISM1 acts as an anti-cancer agent by triggering apoptosis, which helps prevent the proliferation of tumor cells (10, 40, 42). Sahiri et al. (10) investigated the ISM1 expression in several kidney injury models. The levels of ISM1 were significantly increased in DXN-induced nephropathy. Kidney cells injured by DXN may produce more ISM1 protein. This increased production might be part of the tissue's attempt to regulate damage. In the case of ISM1, the increase in its level may be linked to its role in initiating cell death (apoptosis) in podocytes (10).

2.2.2. Zinc-α-Glycoprotein

ZAG is an adipokine secretory protein with a 41-kDa first purified from human plasma by Burgi in 1961 (43). ZAG is not limited to one type of tissue; it is also widely expressed in liver, adipose tissue, kidney, lungs, pancreas, breast, prostate, skin, and glandular tissue, and is then secreted into the body fluid. ZAG has one strong binding site for zinc and 15 weak binding sites. Zinc binding to ZAG protein is critical because it influences the formation of the protein's active form. Zinc-induced oligomerization is important due to its effect on the protein's ability to bind to fatty acids and interact with receptors that promote fat breakdown, such as β-adrenergic receptors. It has a crucial role in protecting against obesity, insulin resistance, hepatic steatosis, and inflammation (11, 12).

Liver and adipose tissues are the two main sites for ZAG synthesis (13). It has an important role in lipid and carbohydrate metabolism (13, 12, 44). A study on human adipose tissue samples reported a positive correlation between insulin sensitivity and the expression of GLUT-4 mRNA and ZAG protein content in subcutaneous adipose tissue. In contrast, a decrease in ZAG levels results in a reduction of IRS1 and GLUT-4 gene expression in primary human adipocytes (13). Likewise, it induces insulin sensitivity and glucose utilization by activating the IRS/AKT signaling pathway. Various studies showed ZAG's role in glucose metabolism by activation of AMPK, which is a key enzyme in cells, regulates energy balance. AMPK activation promotes the translocation of GLUT-4 to the cell surface,

allowing sugar uptake into the cells. This means that ZAG has an indirect effect on blood sugar levels, making it easier for cells to absorb and use glucose (12). Shigefuku et al. (44) have found for the first time that the ZAG serum levels is highly correlated with liver function in patients with chronic liver disease (CLD). Meanwhile, ZAG levels decreased in advanced CLD, which reflects liver dysfunction.

ZAG plays a significant role as a lipid-mobilizing factor in adipose tissue, promoting fat breakdown in adipocytes and influencing weight loss. ZAG helps to maintain a healthy body weight by reducing lipogenesis processes. ZAG treatment has been shown to reduce adipose tissue levels. This phenomenon occurs through the augmentation of lipolysis and the upregulation of non-esterified fatty acids. Consequently, this results in a reduction of plasma TG levels in rats. At the same time, ZAG treatment has also been observed to elevate the levels of adipose triglyceride lipase and hormone-sensitive lipase (HSL), which are involved in lipolysis. Overexpression of ZAG in hepatocytes promotes the lipolysis and β-oxidation of fatty acids and inhibits palmitic acid-induced lipogenesis and lipid accumulation in hepatocytes. Conversely, the downregulation of ZAG expression exhibited a substantial promotion of lipogenesis and increased lipid levels in hepatocytes. There is increasing evidence that ZAG is involved in lipid metabolism; however, the underlying mechanism remains unclear (11-13, 45).

2.3. L-Theanine

LT has a molecular formula ($C_7H_{14}N_2O_3$) with M.W. 174.198 g/mol (16). The other names for it are γ-glutamylethylamide and γ-ethylamino-γ-glutamic acid, and it is commercially known as Suntheanine (15). This non-proteinaceous water-soluble amino acid is found in tea leaves, comprising over 50% of the total free amino acids. The amount of LT differs according to the type of tea and the timing of the harvest. In the early summer period, the amount of LT is the highest compared to the harvest in the late summer season (46). The natural theanine in tea is found in the L-configuration; meanwhile, synthetic theanine is a mixture of D- and L-configuration. The biological activity of LT is higher than D-theanine (47).

LT is biosynthesized in the root of the tea tree from L-glutamic acid and ethylamine by theanine synthetase. After that, LT is transported through the bast and accumulated in the leaves (15, 16). It is responsible for giving tea its distinctive taste (48).

2.3.1. The Effects of L-Theanine on Health

Multiple studies have reported numerous biological and pharmacological activities of LT, including protection against cerebral ischemia/reperfusion injury, antitumor, stress-modulating, antiaging, antianxiety, anti-inflammatory, hepatoprotective, immune-modulating, and neuroprotective effects. The absorption of LT occurs via a sodium-coupled co-transporter located within the intestinal brush margin mucosa. Thereafter, LT works in different tissues and regulates body functions (15, 16).

LT increases the activity of phosphofructokinase in the liver, which helps in glucose breakdown. Meanwhile, LT reduces the activity of phosphoenolpyruvate carboxykinase-1 and glucose-6-phosphatase, which are involved in glucose production in the liver; thus, LT leads to a reduction in glucose production (49).

A pharmacokinetic study reported a lag time of approximately 10 min following LT intake. The half-lives of absorption and elimination were approximately 15 min and 65 min, respectively. LT reached the maximum blood concentration after 50 min. Meanwhile, intragastric administration of LT after 1 h reaches the peak in serum and liver (16).

LT reduces total cholesterol TC, TG, and LDL-C, which are all markers for fat accumulation, and increases HDL-C, which promotes cholesterol clearance by the liver, indicating that LT can modulate lipid metabolism (14, 49, 50). It has been reported that LT supplementation decreased lipoprotein lipase and increased HSL, indicating that it helps protect the body against the accumulation of excess fat (14). LT decreases the levels of SREBP-1c protein in the liver, indicating that it helps control lipid synthesis (49).

LT is either excreted from the body through urine or broken down by enzymes in the kidneys into ethylamine and glutamic acid (16). LT is metabolized to glutamic acid, which is then deprotonated to form glutamate, a key component in GSH synthesis (16, 51).

Many researchers mentioned that LT has the ability to reduce oxidative stress-induced damage via decreasing the production of ROS, lipid damage, and enhancing antioxidant enzymes as well (15). LT was administered to rodents exposed to a chemotherapy drug, and its efficacy was demonstrated in reducing pain, oxidative stress, and inflammation. Since chemotherapy induces oxidative stress, preserving glutathione levels is a pivotal protection against ROS, and treating with LT showed the ability to restore levels of antioxidants, including glutathione. Increasing GSH levels enhances the overall antioxidant

defense system (52). In several studies on LT activity, its effectiveness in reducing the levels of liver enzymes (ALT and AST), MDA, TNF-α, and improving the activities of antioxidant enzymes such as GSH-Px, superoxide dismutase, catalase, and GSH has been reported. Therefore, it is considered proven for LT activity as a Hepatoprotective (5, 53, 54).

3. MATERIALS and METHODS

3.1. Materials

The devices, tools, and materials used in this study are listed in Table 1, the chemicals are listed in Table 2, and the commercial kits are listed in Table 3.

Table 1. Devices, tools, and materials used in the laboratories, and their manufacturers

Devices, Tools and Materials	Manufacturer
Autoanalyzer	Beckman Coulter AU5800 (USA)
Automatic Pipettes	Socorex (Swiss); Isolab (Germany); Ependorf (Germany)
Centrifuge	Eppendorf, Centrifuge 5810 (Germany)
ELISA Washer	Biotek ELx 50 (USA)
Hand Homogenizer	OMNI-Tissue Master 125 (USA)
Magnetic Stirrer	Termal (Türkiye)
Microcentrifuge	Thermo IEC Micromax (USA)
Microcentrifuge Tube	Iso Lab, Lot No: MTPPN7015002 (Germany)
Microplate Reader	Versa Max, Moleculer Devices (USA
Microplate Washer	BioTek ELx50 (USA)
Shaker Incubator	ShelLab/Sheldon S14-2 (USA)
Sonication Device	Sonics Vibra-Cell, 42174L (USA)
Vortex	IKA Vortex, Genius 3 (Türkiye)
Water Purifier	Kros (Türkiye)

Table 2. Chemicals

Chemicals	Manufacturer, Code and Purity
Acetic Acid	Sigma-Aldrich, Lot No: SZBE2190V (USA)
Chloroform	Merck, Cat No: 1.02431 (Germany)
Coomassie Brilliant Blue G-250	Merck, Cas No: 6104-58-1 (Germany)
Ethanol	Merch, Cas No: 64-17-5 (Germany)
KCl	Merch, Cas No: 7447-40-7 (Germany)
Methanol	Merch, Index No: 603-001-00-X (Germany)
NaCl	Sigma-Aldrich, Lot No: SZBE1470V, (99.8%) (USA)
Thiobarbituric Acid (TBA)	Sigma-Aldrich, Lot No: BCCD1032, (≥98%) (USA)
Triton X-100	Sigma, Lot No: SLBP6453V (USA)
Doxorubicin	Bostonchem, Cas No: 25316-40-, (98%) (USA)
L-Theanine	Chem-Impex Intl, Cat No: 14293, (99%) (USA)

FFA, GSH, and GSSG levels were evaluated using the colorimetric assay method. An enzyme-linked immunosorbent assay (ELISA) sandwich method was used for GPx4, TNF-α, Insulin, ISM1, and ZAG, as described in the commercial kit listed in Table 3 below.

Table 3. Commercial kits

Kits	Trademark, Product code, Lot No, City, Country
FFA Kit	Elabscience, E-BC-K013-S, WX07B6J5565 , Texas, USA
Glutathione Kit	Cayman Chemical, 703002, Michigan, USA
GPx4 Kit	BT LAB, E1787Ra, 202402009, Jiaxing, China
TNF-α Kit	BT LAB, E0764Ra, 202402009, Jiaxing, China
Insulin kit	Elabscience, E-EL-R3034, WX03R46H2739, Texas, USA
ISM1 Kit	Shanghai Coon Koon Biotech Co, CK-bio-25542, 202403, Shanghai, China
ZAG Kit	BT LAB, E3313Ra, 202404006, Jiaxing, China

3.2. Methods

Our study was accomplished with the support of the Karadeniz Technical University Scientific Research Project (BAP) named "Investigation of the effect of L-theanine on Glucose and Lipid Metabolism in Rats Treated with Doxorubicin" (Project No: TYL-2024-10980). In addition, the approval (No: date 05.02.2024).

3.2.1. Experimental Groups

In this study, 28 male Wistar rats were obtained from the Karadeniz Technical University Surgical Application and Research Center. The rats weighed 180-220 g and were housed in the center at room temperature, with a 12-h light and 12-h dark cycle, and were provided with standard rat chow and drinking water *ad libitum*. All rats were randomly divided into four groups (n = 7 / group):

Group I (Control): Injected saline and given drinking water.

Group II (DXN): Injected DXN, 18 mg/kg

Group III (DXN +LT200): Injected DXN, 18 mg/kg, and given LT (200 mg/kg/day)

Group IV (DXN +LT400): Injected DXN, 18 mg/kg, and given LT (400 mg/kg/day)

Saline or DXN (dissolved in saline) injections were done intraperitoneally (i.p.) on the 4th, 11th, and 18th days of the 21-day treatment. DXN injections (6 mg/kg/dose) were applied three times (cumulative 18 mg/kg). 200 or 400 mg/kg/day LTs (dissolved in water) were given by oral gavage one hour before the DXN injection, for 21 days (55, 56).

3.2.2. Biochemical Analysis

3.2.2.1. The Parameters Analyzed by the Autoanalyzer

Serum levels of glucose, TG, TC, LDL-C, HDL-C, and liver function markers [lactate dehydrogenase (LDH), ALT, AST], as well as Fe and homocysteine (Hcy), were analyzed using an autoanalyzer (Beckman Coulter Analyzer AU 5800, California, USA) in the Biochemistry Laboratory of Farabi Hospital.

Glucose levels were assessed by the enzymatic hexokinase (HK) / glucose-6-phosphate dehydrogenase (G6P-DH) method. In the presence of ATP, HK phosphorylates glucose to release G6P and ADP. After this, G6P-DH converts G6P to gluconate-6-phosphate. At the same time, nicotinamide adenine dinucleotide (NAD^+) is reduced to

nicotinamide adenine dinucleotide hydride (NADH). An increase in NADH absorbance at 340 nm correlates with glucose concentration.

TG concentrations were evaluated by using the enzymatic colorimetric method with (Glycerol Kinase-Glycerol Phosphate Oxidase-Peroxidase) enzymes. lipoprotein lipase converts TG to glycerol and free fatty acids. Afterward, glycerol is combined with ATP by glycerol kinase, resulting in the production of glycerol-1-phosphate (G-1-P). Then, glycerol phosphate oxidase oxidized G-1-P to dihydroxyacetone phosphate and H_2O_2. Thereafter, peroxidase (POD) catalyzes the reaction of hydrogen peroxide with 4-aminoantipyrine (4-AAP), resulting in the formation of a colored compound known as quinoneimine. The density of quinoneimine absorbance is proportional to TG concentration.

TC levels analysis was done by using an enzymatic colorimetric test (cholesterol oxidase (CHO) - peroxidase). Cholesterol is oxidized by the CHO enzyme releasing H_2O_2. In turn, H_2O_2 reacts with 4-AAP and phenol by POD, yielding a chromophore. The absorbance at 540/600 nm of the produced red quinoneine dye reflects the cholesterol amount in the sample.

LDL-C concentration measured by the enzymatic colorimetric method (CHO - Peroxidase). LDL-C is catalyzed by cholesterol esterase (CHE) and CHO in the presence of (H_2O) and oxygen (O_2), producing Cholest-4-en-3-one (a cholesterol derivative), Fatty acids, and H_2O_2. Then, H_2O_2 is catalyzed by POD, the concentration of LDL-C is calculated by measuring the intensity of the blue color formed.

HDL-C levels were measured by an enzymatic colorimetric test (CHO peroxidase). Starting with the anti-β-lipoprotein antibody binds to lipoproteins other than HDL (LDL-C, VLDL, and chylomicrons). This forms antigen-antibody complexes, isolating these lipoproteins from HDL-C. Subsequently, HDL-C reacts with H_2O and O_2 by CHE and CHO. Producing cholest-4-en-3-one, fatty acids, and H_2O_2. This generated H_2O_2 interacts with the compounds aminoantipyrine and N-ethyl-N-(2-hydroxy-3-sulfopropyl)-3,5-dimethoxyaniline, facilitated by POD, which forms a blue dye. An enzyme-chromogen system determines HDL-C concentration.

LDH levels were evaluated by the kinetic UV Test (IFCC) method. pyruvate is oxidized to lactate by LDH, jointly with the reduction of NAD^+ to NADH. An increase in NADH amount was measured at 340 nm, which is equivalent to LDH activity in the sample.

ALT levels were measured by the kinetic-U.V., pyridoxal-5'-free phosphate method. ALT produces pyruvate and glutamate by transferring the amino group from alanine to 2-oxoglutarate. The catalytic activity of ALT is increased by adding pyridoxal phosphate to the reaction. Following this, LDH facilitates the interaction between pyruvate and NADH, resulting in the formation of lactate and NAD^+. A decrease in the absorbance at 340 nm is correlated with the concentration of ALT in the sample.

AST levels were evaluated with the kinetic-U.V., pyridoxal-5'-free phosphate method. AST facilitates the transamination of aspartate and 2-oxoglutarate, resulting in the production of L-glutamate and oxaloacetate. The AST activity is enhanced by adding pyridoxal phosphate to the reaction. Subsequently, malate dehydrogenase will reduce Oxalacetate to L-malate, concurrently, NADH is converted to NAD^+. The absorbance is measured at 340nm, which reflects AST activity in the sample.

Hcy levels were evaluated by the enzymatic UV method. Hcy S-methyltransferase assists the interaction between Hcy and S-adenosylmethionine, which produces S-adenosylhomocysteine (SAH). Thereafter, in the presence SAH hydrolase is hydrolyzed to adenosine and Hcy. This hydrolysis reaction utilizes NADH and converts it to NAD^+, decreasing in absorbance at 340 nm. This decrease reflects the amount of Hcy in the sample.

Iron levels were measured by using the photometric color test principle. 2,4,6-Tri-(2-pyridyl)-5-triazine (TPTZ) is used as a chromogenic agent. Under acidic conditions, the iron bound to transferrin is released as free iron ions and apotransferrin. This process uses hydrochloric acid and sodium ascorbate to reduce trivalent iron ions to bivalent form. Following this, the bivalent iron ions are merged with TPTZ. As a result, a blue-colored compound was produced and measured dichromatically at 600/800 nm. The absorbance of the emitted color was directly proportional to the iron concentration in the sample.

3.2.2.2. Determination of FFA Levels

The levels of serum FFA in rats were measured by using a commercial kit (Elabscience, Item no: E-BC-K, Texas, USA). FFA levels were detected according to the kit protocol. The absorbance was measured at 450 nm, and the concentration was calculated according to the standard graph shown in Figure 2.

Figure 2. FFA standard curve

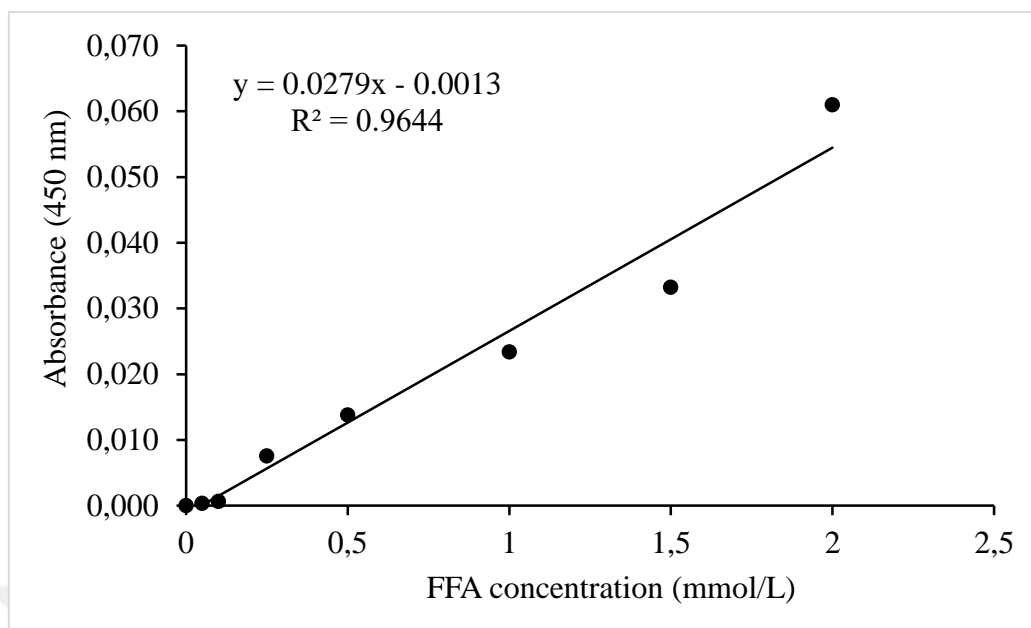### 3.2.2.3. Determination of Insulin Levels

The levels of serum insulin in rats were measured by using a commercial kit (Elabscience, Item no: E-EL-R3034, Texas, USA). Insulin levels were measured according to the kit protocol. The concentration was measured at 450 nm, then insulin levels were calculated according to the standard graph seen in Figure 8.
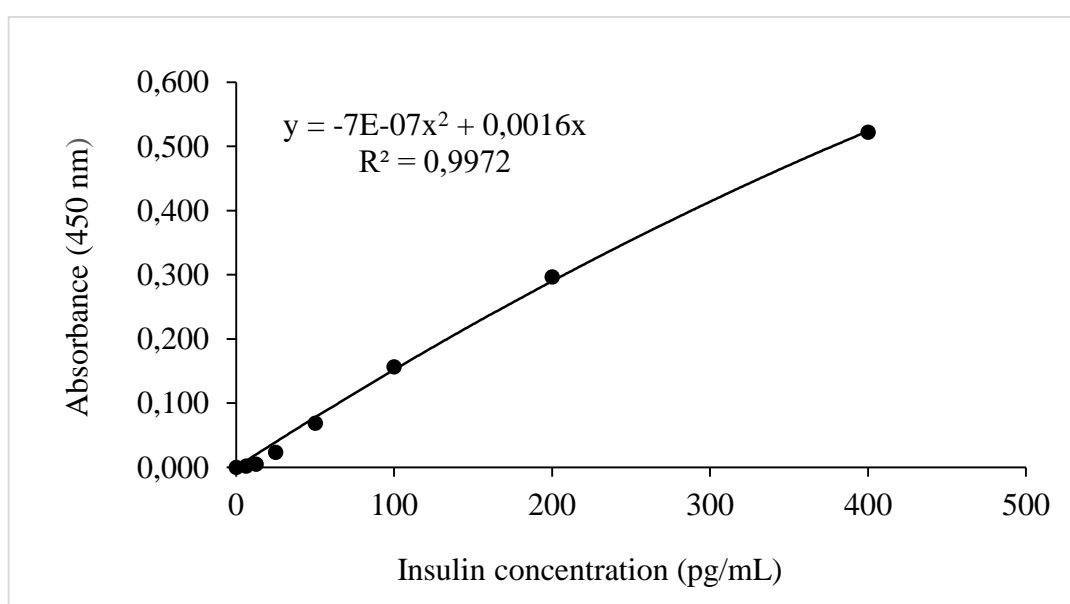

Figure 3. Insulin standard curve

3.2.2.4. Determination of MDA Levels

The evaluation of liver MDA (t-MDA) levels was conducted using the method developed by Mihara and Uchiyama (57). This technique involves determining the absorbance at 532 nm of the color formed when MDA reacts with thiobarbituric acid under acidic conditions.

Tissue Homogenization

For MDA measurement, 50 µg of liver tissue was utilized. The tissue samples were then homogenized on ice with 2 mL of a 1.15% KCl solution that contained 0.5 mL/L TritonX-100.

Solution Preparation

1) 1.15% KCl solution: 5.75 g of KCl salt with 250 µL of TritonX-100 were added to 500 mL of distilled water.

2) 1% phosphoric acid (H_3PO_4) solution: To prepare a 1% H_3PO_4 solution, a volume of 1.176 mL of 85% H_3PO_4 was measured and diluted with distilled water to achieve a total volume of 100 mL.

3) Thiobarbituric acid (TBA) solution: To prepare the TBA solution, 0.335 g of TBA was measured and combined with 25 mL of distilled water. The mixture was agitated using a magnetic stirrer for 30 min. Subsequently, 25 mL of acetic acid was added to the solution.

4) Standard solution: 8.3 mL of tetramethoxypropane was added to a 0.01 M HCl solution and then incubated at 50°C for one h. The prepared 1000nmol/L intermediate stock solution was then used to create standard solutions at concentrations of 100, 50, 25, 12.5, 6.25, 3.125, 1.56, and 0 nmol/mL.

Table 4. Reaction mixture for measuring MDA levels

Reactive	Volume (µL)
Blank	500
1% H_3PO_4 solution	3000
TBA solution	1000
Incubation at 100 ºC for 1 h	
Spectrophotometric measurement at 532 nm	

The mixture described in the table was vortexed (proportions can be adjusted to 500-3000-1000 mL). After incubation, the sample was centrifuged at 4000 rpm for 10 min. Following cooling, the supernatants were pipetted into the ELISA plate and measured by a spectrophotometer at 532 nm. MDA concentration was determined using the standard graph in Figure 3. t-MDA levels were expressed as nmol/mg protein.
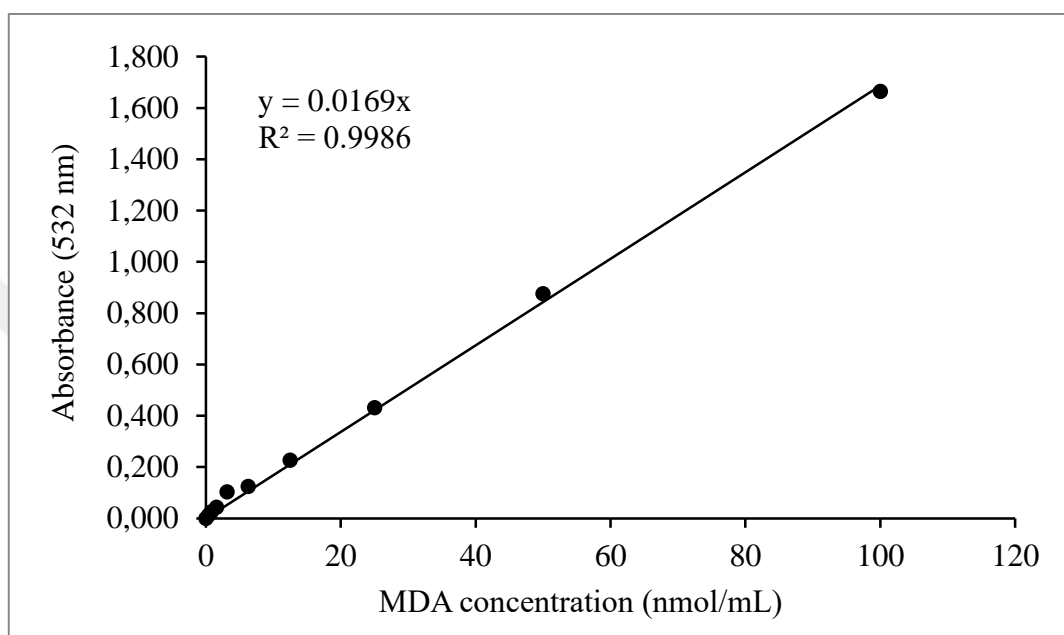

Figure 4. MDA standard curve

3.2.2.5. Determination of Glutathione Levels

Levels of liver total and oxidized glutathione (TGSH and GSSG) were measured by using a commercial kit (Cayman Chemical, Item No: 703002, Michigan, USA). The determination was performed according to the instructions provided in this kit. Firstly, 100 mg of tissue was placed in 1 mL of cold 4-morpholinethanesulfonic acid buffer and then centrifuged at 10,000×g for 15 min at 4 °C to obtain the supernatant. Second, deproteinization was performed using metaphosphoric acid, and triethanolamine was added to the supernatant for TGSH measurement. Then, for GSSG determination, the deproteinized samples were derivatized with 2-vinylpyridine and incubated at room temperature. This step was essential to distinguish GSSG by masking GSH before analysis. Absorbance was measured at 405 nm, and the levels were calculated according to Figures 4 and 5. Liver TGSH and GSSG (t-TGSH and t-GSSG, respectively) levels were given in nmol/mg protein units to standardize.
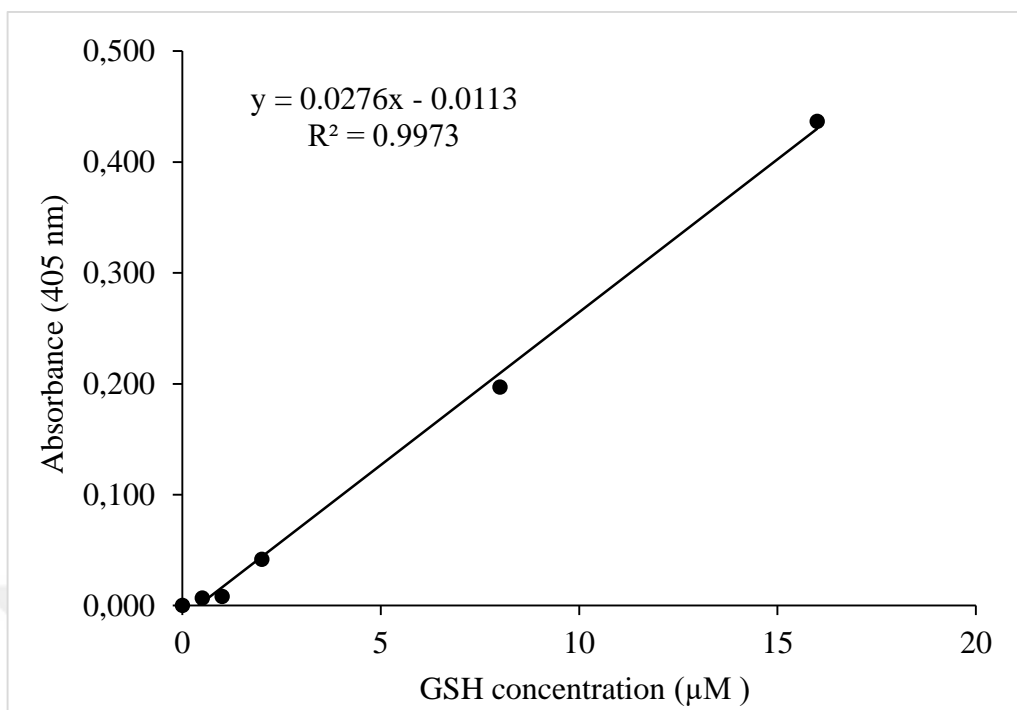
Figure 5. GSH standard curve
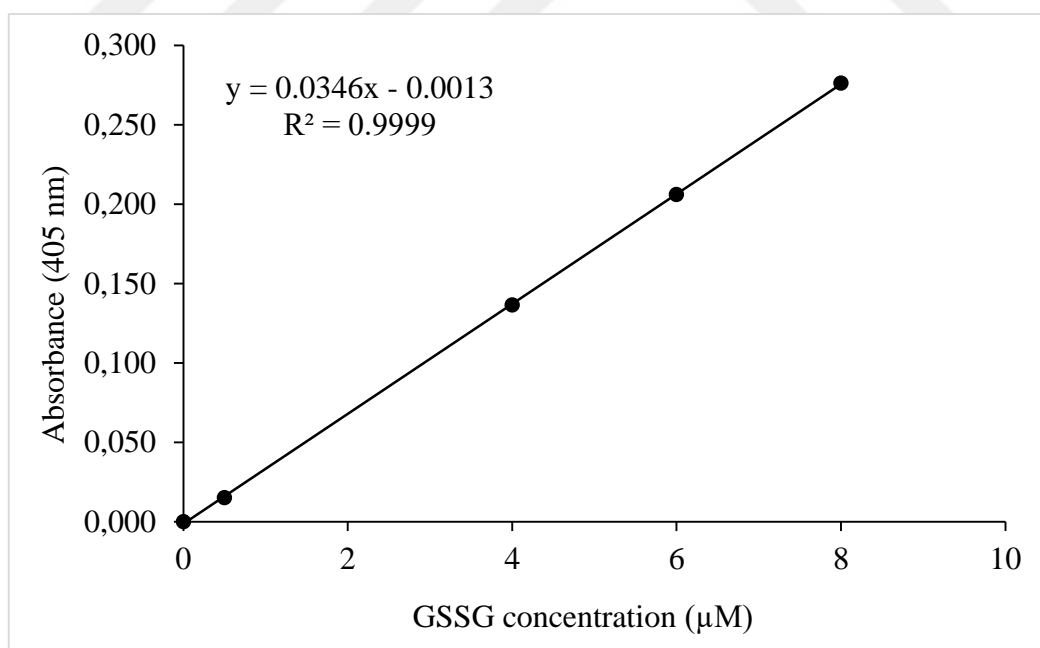
Figure 6. GSSG standard curve

21

3.2.2.6. Determination of GPx4 Levels

The levels of GPx4 in rats' plasma and liver tissue (t-GPx4) were evaluated by using a commercial kit (BT Lab, Item no: E1787Ra, Jiaxing, China) based on Sandwich-ELISA. Tissue homogenization and measurement were performed according to the kit protocol.

Preparation of Homogenate

Tissue was placed in a certain amount of phosphate-buffered saline PBS buffer with a glass homogenizer on ice. After that, the homogenate was centrifuged for 5 min at 5000×g to obtain the supernatant, and the absorbance was measured at 450 nm. t-GPx4 levels were calculated following the standard graph as shown in Figure 6. The levels were given in µU/mg protein units to standardize.

$$y = -2E\text{-}05x^2 + 0.0137x$$
$$R^2 = 0.9962$$
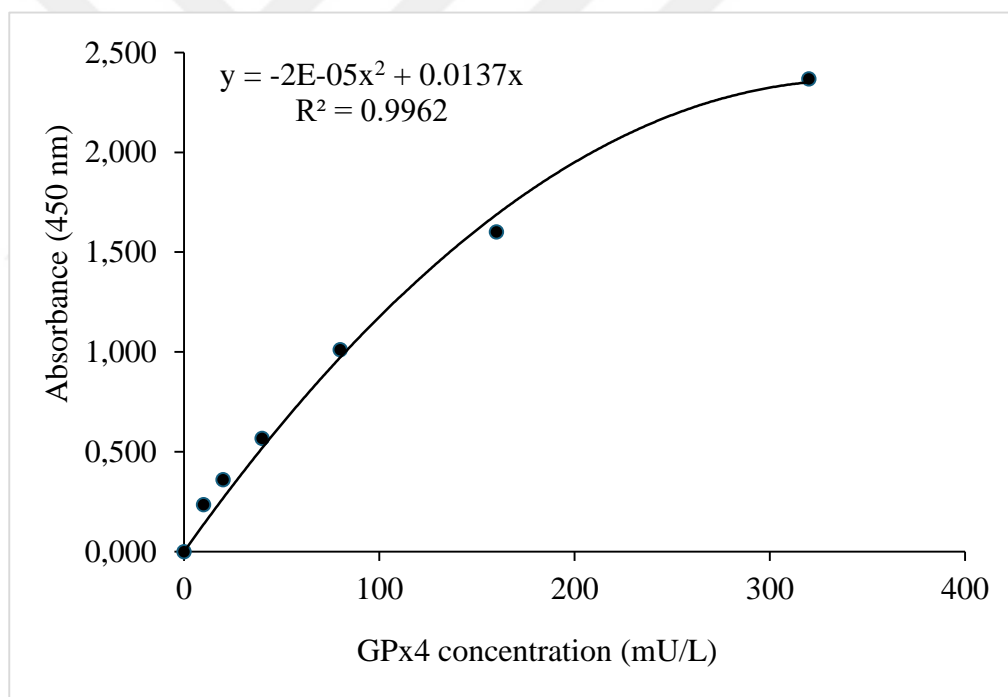
Figure 7. GPx4 standard curve

3.2.2.7. Determination of TNF-α Levels

The levels of TNF-α in rat plasma and tissue (t-TNF-α) were determined by using a commercial kit (BT Lab, Item no: E0764Ra, Jiaxing, China). Tissue homogenization was applied as described in section 3.2.2.6. The levels in the prepared homogenates were determined according to the kit protocol and calculated using the standard graph shown in Figure 7. The levels in the tissues were expressed as ng/L protein unit.
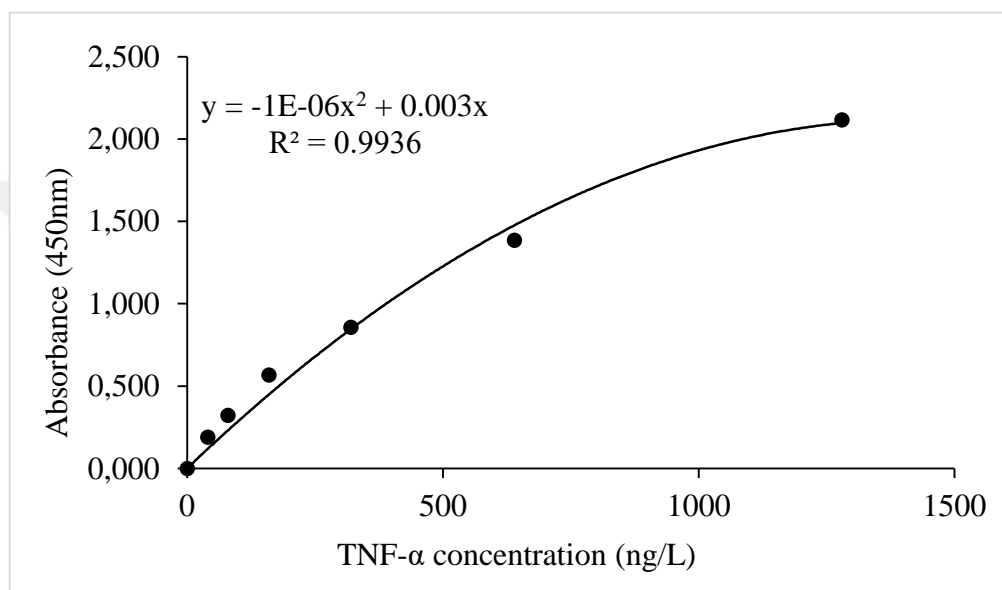
Figure 8. TNF-a standard curve
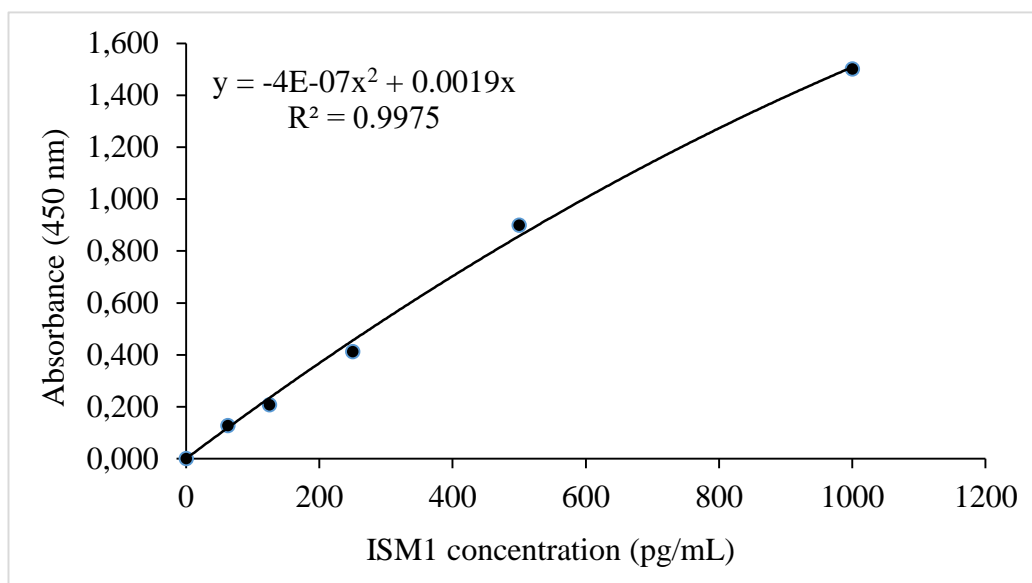
Figure 9. ISM1 standard curve

3.2.2.8. Determination of ISM1 Levels

ISM-1 levels were determined in rats' plasma and liver tissue (t-ISM1) by using a commercial ISM-1 kit (Shanghai Coon Koon Biotech, Item No: CK-bio-25542, Shanghai, China) based on Sandwich-ELISA. Tissue homogenization was applied as described in section 3.2.2.6. The levels in the prepared homogenates were determined according to the kit protocol and calculated using the standard graph shown in Figure 7. The levels in the tissues were expressed as pg/mL protein unit.

3.2.2.9. Determination of ZAG Levels

ZAG levels in rats' plasma and liver tissue (t-ZAG) were measured by using a commercial kit (BT lab, Item no: E3313Ra, Jiaxing, China) based on Sandwich-ELISA. Tissue homogenization was applied as described in section 3.2.2.6. The levels in the prepared homogenates were determined according to the kit protocol and calculated using the standard graph shown in Figure 7. The levels in the tissues were expressed as ng/mL protein unit
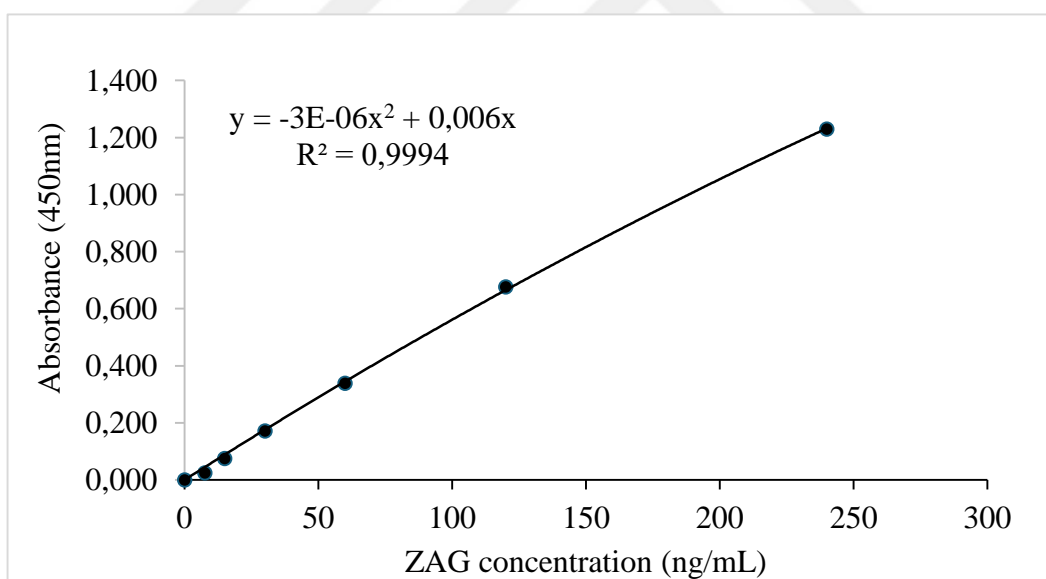

$$y = -3E\text{-}06x^2 + 0,006x$$
$$R^2 = 0,9994$$

Figure 10. ZAG standard curve

3.2.2.10. Determination of Liver TG and TC Levels

The levels of TG and TC in liver tissue (t-TG and t-TC, respectively) were determined by first preparing the tissue homogenate. Briefly, 100 mg of liver tissue was homogenized by adding 500 µL of 1 M NaCl solution. 3 mL of chloroform/methanol (2:1) was also added to the homogenized tissues and incubated overnight in a shaker at room temperature. After that, the homogenate was centrifuged at 3000 × g for 10 min, and the resulting lipid-containing organic subphase was removed. The excess liquid was then evaporated in an oven at 50 ºC. The remaining pellet was dissolved in 220 mL of a 2% Triton X-100 solution containing 1 M NaCl for 15 min, followed by three 5-second sonication cycles. Spin was applied to remove foam.

The t-TG and t-TC content of the sample will be determined by measuring it on an autoanalyzer, as described in section 3.2.2.1.

3.2.2.11. Determination of Total Protein Levels in Liver Tissues

The Bradford method was used to determine protein concentrations in liver tissue homogenates, as described in the steps provided in the commercial kit. This technique relies on the interaction between Coomassie Brilliant Blue G250, an organic dye, and proteins in a phosphoric acid environment. The resulting blue complex exhibits peak absorbance at 600 nm.

<u>**Solution Preparation**</u>

1) Bradford reagent: This reagent was prepared by combining 10 mg of Coomassie Brilliant Blue G-250 with 5 mL of 95% ethanol and 10 mL of 85% H_3PO_4. The final volume was brought to 100 mL using distilled water.

2) Standards: The bovine serum albumin standards were created with concentrations ranging from 0 to 1 mg/mL (1, 0.9, 0.8, 0.7, 0.6, 0.5, 0.4, 0.3, 0.2, 0.1, 0.05, 0.025, and 0 mg/mL). The Bradford method's sensitivity ranges from 1 to 100 µg. Consequently, liver samples were diluted 30-fold with distilled water for t-MDA measurement and 80-fold for t-TG and t-TC measurements. The results obtained by pipetting are provided in Table 5. Absorbance was read at 600 nm, and the albumin concentration was calculated using the reference standard curve shown in Figure 11.

Table 5. Material measurement for the protein levels determination

	Blank (µL)	Standard (µL)	Sample (µL)
Blank	10	-	-
Standard	-	10	-
Sample	-	-	10
Bradford Reagent	100	100	100
Incubated at room temperature for 10 min, and the absorbance was read at 600 nm.			
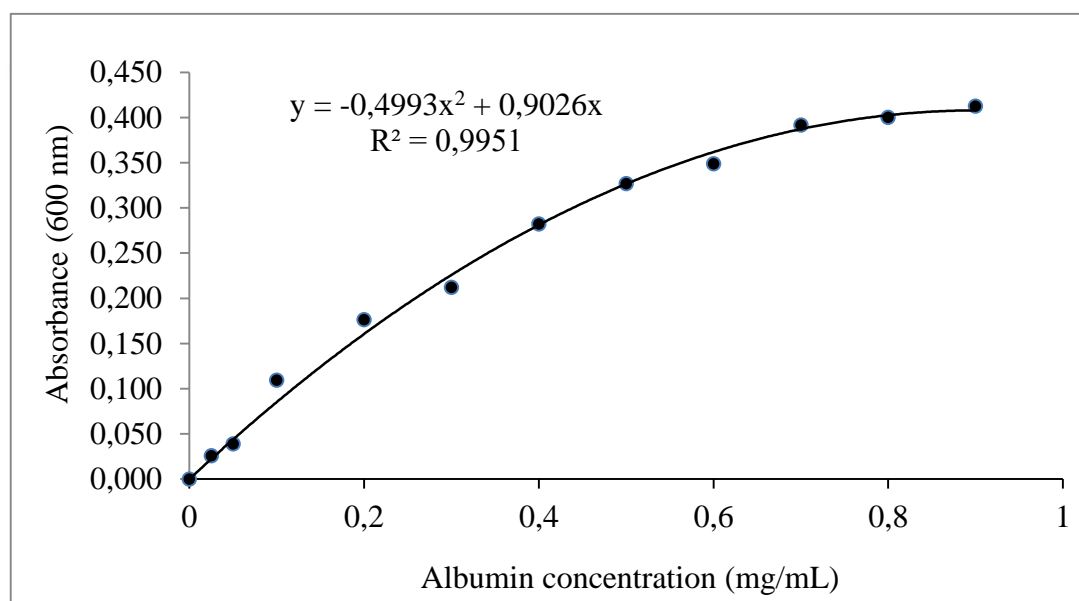
Figure 11. Standard curve for protein concentration

The plotted equation: $y = -0,4993x^2 + 0,9026x$, $R^2 = 0,9951$

3.2.3. Statistical Analysis

Our data were evaluated statistically by using the SPSS (IBM SPSS Statistics 23) program. The conformance for the normal distribution of our parameters was understood by applying "Shapiro-Wilk" test. To compare two variables that did not fit the normal distribution, the "Mann-Whitney U" test was used, while the "Student's t" test was used for two variables that fit the normal distribution. Moreover, the "Kruskal-Wallis" test was used to compare more than two variables that did not fit the normal distribution, and "One-Way ANOVA" was used to compare more than two variables that fit the normal distribution. For post hoc evaluation, the "Tukey" test was used. Parametric results were given as "mean ± SD", and p values were given according to "One-Way ANOVA"; however, non-parametric results were given as "Median [IQR] and 25th-75th percentiles" and p values according to 'Kruskal-Wallis' test.

4. RESULTS

4.1. Animal Weights

The initial and final weights of the rats are shown in Table 6. After 28 days of administering the medications, it was observed that the body weights of the rats in both the DXN and LT treatment groups were lower than those in the control group ($p < 0.05$). However, LT treatment did not significantly affect the weight of rats treated with DXN.

Table 6. The body weight of the study groups

	Control (n=7)	DXN (n=7)	DXN+LT200 (n=7)	DXN+LT400 (n=7)	p
Initial Weight (g)	190 [9] (185-194)	181 [1] (181-182)	181 [7] (180-187)	180 [8] [a] (178-186)	0.040
Final Weight (g)	240 ± 16	154 ± 7 [a]	158±20 [a]	131 ± 65 [a]	0.000

Parametric results were given as "mean ± SD" and p values were given according to the One-Way ANOVA test. Non-parametric results were given as "Median [IQR] and 25th -75th percentiles" and p values according to 'Kruskal-Wallish' test. $p < 0.05$ was statistically significant with respect to [a]: control.

4.2. Biochemical Results

According to Tables 5 and 6, the biochemical results showed no significant difference in TG, AST, LDH, TNF-α, GPx4, ISM1, MDA, t-ZAG, t-TGSH, and t-TGSSG among the study groups ($p > 0.05$). However, Hcy and insulin levels were significantly lower in DXN, LT200, and LT400 groups compared to the control group ($p < 0.05$). Meanwhile, TC, LDL-C, HDL-C, ALT, Fe, t-TNF-α, t-GPX4, and t-ISM1 levels showed a significant increase between the groups when compared to the control group ($p < 0.05$). ZAG significantly decreased in the DXN+LT400 group compared to all other groups.

Table 7. Comparisons of the results of plasma and serum biochemical parameters between study groups

	Control (n=7)	DXN (n=7)	DXN+LT200 (n=7)	DXN+LT400 (n=7)	p
Glucose (mg/dL)	113 [17] (107 – 124)	150 [48] (118 – 166)	133 [31] (131 – 162)	122 [28] (100 – 128)	0.057
TG (mg/dL)	79 [24] (65 – 89)	88 [131] (78 – 209)	102 [49] (82 – 131)	90 [51] (72 – 123)	0.226
TC (mg/dL)	47.7 ± 6.6	91.9 ± 17.3 [a]	85.9 ± 15.5 [a]	87.8 ± 16.2 [a]	0.000
LDL -C (mg/dL)	18.9 ± 4.3	40.7 ± 8.3 [a]	35.1 ± 7.9 [a]	33.6 ± 5.7 [a]	0.000
HDL -C (mg/dL)	31.3 ± 3.5	50.3 ± 6.4 [a]	49.7 ± 8.1[a]	50.8 ± 12.2 [a]	0.001
FFA (mmol/L)	1.54 [0.10] (1.52 - 1.62)	1.54 [0.09] (1.51 - 1.60)	1.57 [0.07] (1.52 - 1.59)	1.64 [0.10] (1.58 - 1.68)	0.335
ALT (U/L)	30 [4] (28 – 32)	50 [76] [a] (49 – 125)	43 [21] [a] (34 – 55)	60 [18] [a] (47 – 65)	0.004
AST (U/L)	134 ± 29	239 ± 101	157 ± 36	165 ± 42	0.170
LDH (U/L)	1034 ± 326	753 ± 392	628 ± 98	771 ± 227	0.082
Fe (µg/dL)	160 [19] (142 – 161)	353 [43] [a] (325 – 368)	299 [92] [a] (242 – 334)	258 [76] [a,b] (219 – 295)	0.000
Hcy (µmol/L)	9.1 ± 2.2	3.9 ± 0.9 [a]	3.0 ± 0.4 [a]	4.0 ± 1.2 [a]	0.000
GPX4 (mU/L)	29.2 [15.2] (28.4 - 43.6)	28.4 [12.0] (24.8 - 36.8)	30.0 [3.4] (28.4 - 31.8)	36.4 [9.1] (30.7 - 39.8)	0.433
TNF-α (ng/L)	108 [27] (92 – 119)	103 [20] (88 – 108)	103 [30] (91 – 121)	120 [39] (98 – 137)	0.388
Insulin (pg/mL)	3750 [642] (3501 – 4143)	388 [138] [a] (348 – 486)	488 [768] [a] (181 – 949)	623 [1424] [a] (379 – 1893)	0.003
ISM1 (pg/mL)	740 ± 25	858 ± 104	869 ± 62	868 ± 152	0.067
ZAG (ng/mL)	24.9 ± 4.5	26.1 ± 7.2	24.9 ± 4.7	15.4 ± 6.2 [a,b,c]	0.029

Parametric results were given as "[Mean ± SD]" and p values were given according to One-Way ANOVA test. Non-parametric results were given as "Median [IQR] and 25th -75th percentiles" and p values according to 'Kruskal-Wallish' test. $p < 0.05$ was accepted statistically significant with respect to [a]: control, [b]: DXN and [c]: DXN + LT200.

Table 8. Comparisons of the results of biochemical parameters in the tissues between study groups

	Control (n=7)	DXN (n=7)	DXN+LT200 (n=7)	DXN+LT400 (n=7)	p
t-TG (mg/mL)	9.2 [4.3] (6.8 - 11.1)	13.3 [7.5] [a] (11.9 - 19.4)	6.5 [5.2] [b] (5.0 - 10.2)	6.9 [8.5] [b] (5.0 - 13.5)	0.007
t-TC (mg/mL)	2.1 [1.1] (1.6 - 2.7)	3.8 [1.5] [a] (3.4 - 4.9)	1.7 [1.1] [b] (1.5 - 2.6)	2.2 [1.8] [b] (2.0 - 3.8)	0.001
t-MDA (nmol/mg)	1.8 ± 0.5	1.7 ± 0.2	1.2 ± 0.2	1.9 ± 0.7	0.078
t-GSSG (nmol/mg)	6.13 [4.22] (5.2 - 9.4)	7.9 [3.7] (4.5 - 8.2)	7.3 [10.2] (2.5 - 12.7)	5.8 [5.2] (4.7 - 9.9)	0.996
t-TGSH (nmol/mg)	19.6 [9.9] (16.0 - 25.9)	23.4 [6.6] (19.0 - 25.6)	22.6 [7.0] (19.5 - 26.5)	20.4 [6.0] (17.7 - 23.7)	0.415
t-GSSG\GSH	0.34 ± 0.13	0.33 ± 0.10	0.33 ± 0.18	0.36 ± 0.12	0.977
t-GPx4 (µU/mg)	4.4 ± 0.8	6.9 ± 2.3 [a]	6.3 ± 2.0 [a]	5.5 ± 1.4 [a]	0.049
t-TNF-α (pg/mg)	13.9 ± 2.6	20.2 ± 7.0	23.2 ± 6.2 [a]	20.8 ± 2.9 [a]	0.031
t-ISM1 (pg/mg)	50 [4] (48 – 52)	97 [40] [a] (62 – 102)	87 [45] [a] (67 – 112)	60 [20] [a] (58 – 78)	0.004
t-ZAG (ng/mg)	3.6 [0.9] (3.5 - 4.4)	5.6 [4.4] (3.4 - 7.8)	5.3 [3.3] (4.0 - 7.3)	4.1 [0.7] (3.7 - 4.4)	0.074

The levels of tissue parameters were expressed per mg protein. Parametric results were given as "[Mean ± SD]" and p values were given according to One-Way ANOVA test. Non-parametric results were given as "Median [IQR] and 25th -75th percentiles" and p values according to 'Kruskal-Wallish' test. $p < 0.05$ was accepted statistically significant with respect to [a]: control and [b]: DXN.

5. DISCUSSION

In our study, we investigated the modulatory effects of LT on glucose and lipid metabolism in rats exposed to (DXN)-induced toxicity. The results exhibit that LT supplementation, especially at higher doses, has a protective effect on several metabolic and biochemical parameters affected by DXN administration.

In our study, serum glucose levels were insignificantly increased following DXN treatment ($p > 0.05$) (Table 7). There is a documented association between DXN treatment and elevated glucose levels (58). DXN is known to cause impairment in glucose metabolism through multiple mechanisms, including the induction of insulin resistance and pancreatic β-cell dysfunction (59). It has been suggested that the primary mechanism of DXN toxicity in pancreatic β-cells is DNA damage, rather than the H_2O_2 produced through the redox cycle (59). Previous studies have demonstrated that DXN modulates insulin signaling pathways by downregulating the AMPK pathway and facilitating GLUT-4 translocation (6, 60). Disturbance in insulin levels leads to impairment in glucose utilization (31). In our study, we observed that DXN decreased insulin levels ($p < 0.05$) (Table 7). This is because of the possibility of DXN-induced pancreatic damage. On the other hand, LT supplementation decreased glucose levels while increasing insulin levels insignificantly. This suggests that LT may counteract the effects of DXN. It has been mentioned in other studies that LT has ability to improve insulin sensitivity, thus enhancing the restoration of the metabolic balance (52).

In our study, DXN treatment increased TG and TC levels in serum and liver tissue, but the effect on serum TG was not significant. in addition, serum LDL-C and HDL-C levels increased significantly ($p > 0.05$) (Table 7). Meanwhile, FFA levels remained unaffected. Similar to our result, it was reported that DXN treatment decreased body weight but increased blood glucose and lipid levels (61). Similarly, another study also reported that decreasing body weight was associated with increased serum TG levels, and they suggested that DXN treatment contributes to an increase in atherogenic dyslipidemia (58). DXN inhibits PPARγ and may cause lipotoxicity in cells (61). The accumulation of cholesterol in pancreatic β cells can affect insulin granules and alter their fusion dynamics, thereby impairing insulin release (62). In addition, DXN causes an increase in ROS production, which in turn stimulates the apoptotic process. These changes decrease insulin production and release by disrupting ATP-sensitive potassium channels (K-ATP) (62). As shown in our

results, LT did not affect lipid metabolism compared to the DXN-induced dyslipidemia (Table 7). Contrary to our findings, another study demonstrated more pronounced lipid-lowering effects of LT when using higher doses or longer treatment durations. A decrease in serum TG and LDL-C levels was reported after LT supplementation in rats with induced metabolic dysfunction. This may indicate that the effects of LT on serum lipid-modulation may depend on other factors such as disease model, treatment dosage, or duration (14). Meanwhile, Saeed et al. (53) reported a moderate LT-induced lipid-lowering effect.

Concurrently, in conjunction with LT supplementation, t-TG and t-TC levels exhibited a substantial decline in comparison to the DXN group ($p < 0.05$) (Table 8). As reported by Saeed et al. (53), the administration of LT led to a reduction in hepatic lipid accumulation and an enhancement in lipid metabolism. A decline in t-TG levels was observed in the LT treatment group in comparison with the DXN group. This finding suggests that LT may effectively diminish DXN-induced lipid accumulation in tissues.

FFA levels showed no significant differences among all the groups ($p > 0.05$) (Table 7). This may indicate that DXN-induced lipid dysregulation did not significantly affect FFA levels in our model. Similarly, LT did not improve FFA levels. In a previous study, DXN has been shown to interfere with TG metabolism, resulting in TG hydrolysis in adipose tissues. Therefore, increases TG and FFA in the blood (63). On the other hand, LT supplementation has been reported to improve lipid metabolism and reduce lipolysis-related markers (53); however, it did not affect FFA levels in either dose in our model.

As we analyzed serum hepatocellular biomarkers, we observed a significant elevation in ALT levels ($p < 0.05$), but no significant differences were observed in AST and LDH levels in DXN compared to the control group ($p > 0.05$) (Table 7), Our results are consistent with Ozturk et al. (25) who reported that ALT elevation after DXN treatment is due to oxidative stress–mediated structural damage as the release of cytosolic liver components typically indicates compromised integrity of hepatocyte membranes Nagai et al. (5) LDH is known to be a key enzyme for the energy production process in cancer cells. It plays a critical role in tumor progression, as it contributes to anaerobic metabolism. It has been reported that patients with elevated LDH levels had a poor response to chemotherapy (64). Neither dose of LT has a significant reduction effect on ALT levels compared to the DXN group, especially at the lower dose. This may indicate a hepatoprotective limited impact, which may depend on the dose and treatment duration. Meanwhile, supplementation

with LT at a lower dose (200 mg/kg) reduced AST and LDH levels compared to the DXN group, but this difference was insignificant (Table 7), which may indicate a dose-dependent protective effect of LT in our model. This may also indicate that LT has a partial protective effect on liver function, as reported by Saeed et al. (53) and Nagai et al. (5) that AST was mildly reduced with LT in chemically induced liver injury. The observed discrepancy between our results and previous studies may be due to differences in treatment duration or dose. Moreover, co-treatment with LT attenuated the elevation of LDH levels induced by DXN-related hepatic injury (65).

We observed an increase in Fe levels in DXN compared to the control (p < 0.05) (Table 7). This elevation in iron levels may be due to some mechanisms of DXN-induced toxicity. DXN-induced ROS production. ROS react with iron, producing a highly toxic hydroxyl radical. This oxidative stress leads to cell death by damaging DNA, proteins, and lipids. Furthermore, DXN has been shown to elevate iron levels by inhibiting IRP-1. This protein has been shown to regulate the expression of genes involved in iron metabolism and homeostasis. Its inhibition results in increased iron levels, thereby promoting oxidative stress. DXN enhances the activity of the ubiquitin–proteasome system (UPS), thereby accelerating intracellular protein degradation and promoting the breakdown of critical cellular proteins (61). This is similar to previously mentioned mechanisms in which DXN disrupts cellular iron homeostasis, releasing iron from stores and promoting oxidative stress through Fenton reactions (4, 66). Iron overload can exacerbate reactive oxygen species (ROS) production, resulting in increased tissue damage and organ dysfunction (4). The results of co-treatment with LT showed that the higher dose had a noticeable effect, which was observed by a significant difference between the DXN+LT400 and DXN groups (p < 0.05). This result may suggest that LT is showing iron-chelating or regulatory effects that alleviate the DXN-induced iron overload. A previous study stated that LT exhibits iron-lowering effects (67).

In our study, treating with DXN significantly reduced plasma Hcy levels in all the groups compared to control group (p < 0.05) (Table 7). Hcy is an important metabolite of methionine (Met), which is an essential amino acid that plays a crucial role in various biological processes within the body, including the transfer of a methyl group (68). Methionine serves as a precursor for the synthesis of cysteine, which contributes to the production of glutathione and helps maintain redox homeostasis through the transsulfuration

pathway. When methionine is oxidized by ROS, it must be reduced to restore its original function (68, 69). Our results indicate that decreased Hcy levels may suggest that DXN upregulates the transsulfuration pathway as a compensatory response to oxidative stress, promoting the conversion of Hcy into cysteine and glutathione. However, a previous study reported that DXN induced mild hyperhomocysteinemia, which may indicate that DXN interferes with methionine metabolism. This interference could lead to increased oxidative stress, which is known to cause alterations in Hcy homeostasis (70). Moreover, it has been mentioned that there has been a reduction effect of LT on Hcy levels in diabetic rats, this effect may stem from LT's capacity to lower methionine levels in the serum, thereby disrupting the formation of Hcy (67). As seen in Table 7, our results showed an inverse trend; LT supplementation has no impact on Hcy levels. The results indicate that LT may not alter Hcy metabolism in our model. As mentioned above, DXN diminished Hcy levels, which may indicate limited efficiency in hepatic tissue injury.

DXN activates the Nrf2 signaling pathway, which in response induces the production of antioxidant proteins to reduce ROS accumulation (71, 72). Meanwhile, as we observed, the elevation antioxidant enzyme t-GPx4 levels may be an indicator of the compensatory effect of Nrf2 activation against DXN-induced oxidative stress (73). Increased iron levels may lead to an increase in oxidative stress; however, elevated t-GPx4 levels may have a mitigating effect on oxidative stress. Therefore, our insignificant change in t-MDA and TGSSG/TGSH levels (Table 8) in the DXN group may be attributed to this effect. Moreover, it has been reported that LT can improve hepatocyte antioxidant capacity by inhibiting MDA formation and increasing the activity of antioxidant enzymes (15). Other studies have shown the opposite of our results; t-MDA levels in the tissues were increased in the DXN group due to DXN-induced oxidative stress, then, decreased with LT supplementation (74, 75). Additionally, no significant change was obtained in t-TGSH and t-GSSG levels in DXN group compared to the control group. While our findings may seem diverse from the well-established oxidative stress-inducing profile of DXN, however, the elevation in t-TGSH levels by DXN was investigated before (76). Hepatocytes, as a self-protective adaptation to oxidative stress, may induce upregulation of glutamate–cysteine ligase, which is the rate-limiting enzyme in GSH synthesis (22).

LT treatment did not affect oxidative stress parameters or antioxidant parameters (Tables 7 and 8). However, the antioxidant and hepatoprotective effects of LT have been reported previously (15, 16).

TNF-α serum levels showed no significant differences between all the groups (p > 0.05) (Table 7). This may suggest that TNF-α levels are neither affected by DXN-induced inflammation in our model nor modulated by LT co-treatment. Meanwhile, it has been reported that LT has anti-inflammatory effects and alleviates TNF-α levels (77). On the contrary, in the tissue, there was an increase in t-TNF-α levels in all the groups, but it was significantly higher in the LT groups with both doses compared to the control group (p < 0.05) (Table 8). The increase in t-TNF-α levels may be due to DXN, which enhances ROS production, leading to activation of the NF-κB pathway; therefore, increased t-TNF-α levels (78). Our reported increase in ALT and AST levels may confirm the occurrence of tissue dysfunction due to the DXN treatment, as indicated by our evaluated results of t-TNF-α. Meanwhile, LT co-treatment did not show a protective effect on t-TNF-α levels. This is proportionate to Arıkan Malkoç et al. (75) finding, which may suggest that the LT supplementation did not help improve treatment and reduce DXN-induced toxicity in the body, as the levels of TNF-α increased in both doses, especially in the lower dose.

Serum ISM1 levels among the groups (Table 7) showed no significant difference (p > 0.05). However, DXN slightly increased ISM1 levels. Meanwhile, there was a statistically significant increase in t-ISM1 levels in DXN compared to the control group (p < 0.05) (Table 8). Jiang et al. (39) and Wang et al. (8) reported an elevation of ISM1 in response to metabolic stress, suggesting that this increase is an adaptive upregulation aimed at restoring glucose and lipid homeostasis. LT treatment showed a decrease in ISM1 levels compared to DXN, although the difference was not statistically significant. In the LT400 dose group, ISM1 levels decreased more than in the LT200 group, but remained higher than in the control group. This finding may indicate that the effectiveness of LT is dose-dependent, with LT400 demonstrating a higher degree of efficacy. In a related experimental context, ISM1 levels were increased in the DXN-treated group in cultured podocytes with no significant increases in its receptors (GRP 78). This led them to conclude that the increase in ISM1 in the DXN-treated group did not stimulate apoptosis (10).

ZAG levels in the blood serum, as shown in Table 7, there was an insignificant increase in ZAG levels following DXN treatment; meanwhile, there was a significant

decrease between the DOX+LT400 group compared to other groups ($p < 0.05$). This may indicate that a potential dose-specific effect of LT on circulating ZAG levels exists with the higher dose (400 mg/kg), which could be considered an indicator of the LT effect on glucose and lipid metabolism. Although a slight elevation in t-ZAG levels was observed following DXN treatment and appeared to decline with LT administration, these changes were not statistically significant ($p > 0.05$) (Table 8). Although ZAG is known as an anti-inflammatory adipokine, it may be upregulated in response to some conditions, including inflammation, oxidative stress, and lipid dysregulation (78). DXN is known to induce these three conditions, which may explain this moderate elevation in both serum and tissue ZAG levels in the DXN and DXN+LT200 groups.

Several limitations should be considered when interpreting the results of this study. The short treatment duration of LT may not have allowed it to fully treat the condition. Dose range restriction: only two doses of LT (200 and 400 mg/kg) were tested. Having a wider range of doses might help us better understand how the dose affects the response. Limited inflammatory and oxidative markers; only a few of the inflammatory and oxidative stress markers were evaluated. Including additional markers could offer a more comprehensive picture. On the other hand, this study also has its strengths. To the best of our knowledge, ZAG and ISM1 levels were first identified in terms of metabolic dysfunction and oxidative stress conditions in DXN-treated animals, as well as in the effects of LT on DXN-treated animals.

In conclusion, DXN has adverse effects on several metabolic parameters, including mild hyperglycemia, dyslipidemia, elevated hepatic enzymes, iron overload, and alterations in homocysteine and inflammatory marker levels. LT supplementation, particularly at a higher dose (400 mg/kg), demonstrated partial alleviation, as evidenced by the improvements in hepatic lipid content, insulin levels, and a reduction in iron accumulation. However, LT showed limited or insignificant effects on other parameters such as serum lipid profile, oxidative stress markers, inflammatory cytokines (TNF-α), and adipokines (ZAG and ISM1). Overall, LT has the potential to counteract certain aspects of DXN-induced metabolic dysfunction.

6. REFERENCES

1. Prasanna PL, Renu K, Valsala Gopalakrishnan A (2020). New molecular and biochemical insights of doxorubicin-induced hepatotoxicity. Life Sci. 250:117599.

2. Mattioli R, Ilari A, Colotti B, Mosca L, Fazi F, Colotti G (2023). Doxorubicin and other anthracyclines in cancers: activity, chemoresistance and its overcoming. Mol Aspects Med. 93:101205.

3. Renu K, Pureti LP, Vellingiri B, Gopalakrishnan AV (2021). Toxic effects and molecular mechanism of doxorubicin on different organs – an update. Toxin Rev. 41(2):650–674

4. Christidi E, Brunham LR (2021). Regulated cell death pathways in doxorubicin-induced cardiotoxicity. Cell Death Dis. 12(4):1–15.

5. Nagai K, Oda A, Konishi H (2015). Theanine prevents doxorubicin-induced acute hepatotoxicity by reducing intrinsic apoptotic response. Food Chem Toxicol. 78:147–152

6. Arunachalam S, Tirupathi Pichiah PB, Achiraman S (2013). Doxorubicin treatment inhibits PPARγ and may induce lipotoxicity by mimicking a type 2 diabetes-like condition in rodent models. FEBS Lett. 587(2):105–110.

7. Pera EM, Kim JI, Martinez SL, Brechner M, Li SY, Wessely O, De Robertis EM (2002). Isthmin is a novel secreted protein expressed as part of the Fgf-8 synexpression group in the xenopus midbrain-hindbrain organizer. Mech Dev. 116(1-2):169–172.

8. Wang J, Du J, Ge X, Peng W, Guo X, Li W, Huang S (2022). Circulating ISM1 reduces the risk of type 2 diabetes but not diabetes-associated NAFLD. Front Endocrinol. 13:890332.

9. Liang JY, Wei HJ, Tang YY (2024). Isthmin: a multifunctional secretion protein. Cytokine. 173:156423.

10. Sahiri V, Caron J, Roger E, Desterke C, Ghachem K, Mohamadou I, Serre J, Prakoura N, Fellahi S, Placier S, et al. (2023). The angiogenesis inhibitor Isthmin-1 (ISM1) is overexpressed in experimental models of glomerulopathy and impairs the viability of podocytes. Int J Mol Sci. 24(3):2723.

11. Wei X, Liu X, Tan C, Mo L, Wang H, Peng X, Deng F, Chen L (2019). Expression and function of zinc-α2-glycoprotein. Neurosci Bull. 35(3):540–550.

12. Severo JS, Morais JBS, Beserra JB, Dos Santos LR, de Sousa Melo SR, de Sousa GS, de Matos Neto EM, Henriques GS, do Nascimento Marreiro D (2020). Role of zinc in

zinc-α2-glycoprotein metabolism in obesity: a review of literature. Biol Trace Elem Res. 193(1):81–88.

13. Namkhah Z, Naeini F, Ostadrahimi A, Tutunchi H, Hosseinzadeh-Attar MJ (2021). The association of the adipokine zinc-alpha2-glycoprotein with non-alcoholic fatty liver disease and related risk factors: A comprehensive systematic review. Int J Clin Pract. 75(7):e13985.

14. Chen X, Chen L, Qin Y, Mao Z, Huang Z, Jia G, Zhao H, Liu G (2022). Dietary L-theanine supplementation improves lipid metabolism and antioxidant capacity in weaning piglets. Anim Biotechnol. 33(7):1407–1415.

15. Saeed M, Khan MS, Kamboh AA, Alagawany M, Khafaga AF, Noreldin AE, Qumar M, Safdar M, Hussain M, Abd El-Hack ME, Chao S (2020). L-theanine: an astounding sui generis amino acid in poultry nutrition. Poult Sci. 99(11):5625–5636.

16. Chen S, Kang J, Zhu H, Wang K, Han Z, Wang L, Liu J, Wu Y, He P, Tu Y, Li B (2023). L-Theanine and immunity: a review. Molecules. 28(9):3846.

17. Sritharan S, Sivalingam N (2021). A comprehensive review on the time-tested anticancer drug doxorubicin. Life Sci. 278:119527.

18. Cancer Research UK (2023, Nov 21). Doxorubicin. Cancer Research UK.

19. Kciuk M, Gielecińska A, Mujwar S, Kołat D, Kałuzińska-Kołat Ż, Celik I, Kontek R (2023). Doxorubicin—an agent with multiple mechanisms of anticancer activity. Cells. 12(4):659.

20. Rayner DM, Cutts SM (2014). Anthracyclines. In: Side Effects of Drugs Annual, Vol. 36, pp. 683–694. Elsevier.

21. Renu K, KB S, Parthiban S, SS, George A, PB TP, Suman S, VG A, Arunachalam S (2019). Elevated lipolysis in adipose tissue by doxorubicin via PPARα activation associated with hepatic steatosis and insulin resistance. Eur J Pharmacol. 843:162–176.

22. Zhang W, Liu Y, Liao Y, Zhu C, Zou Z (2024). GPX4, ferroptosis, and diseases. Biomed Pharmacother. 174:116512.

23. Vašková J, Kočan L, Vaško L, Perjési P (2023). Glutathione-related enzymes and proteins: a review. Molecules. 28(3):1447.

24. Georgiou-Siafis SK, Tsiftsoglou AS (2023). The key role of GSH in keeping the redox balance in mammalian cells: mechanisms and significance of GSH in detoxification via formation of conjugates. Antioxidants. 12(11):1953.

25. Özturk N, Ceylan H, Demir Y (2024). The hepatoprotective potential of tannic acid against doxorubicin-induced hepatotoxicity: insights into its antioxidative, anti-inflammatory, and antiapoptotic mechanisms. J Biochem Mol Toxicol. 38(8):e23798.

26. Buday K, Conrad M (2020). Emerging roles for non-selenium containing ER-resident glutathione peroxidases in cell signaling and disease. Biol Chem. 402(3):271–287.

27. Dar NJ, John U, Bano N, Khan S, Bhat SA (2024). Oxytosis/Ferroptosis in neurodegeneration: the underlying role of master regulator glutathione peroxidase 4 (GPX4). Mol Neurobiol. 61(3):1507–1526.

28. Jang DI, Lee AH, Shin HY, Song HR, Song HR, Park JH, Kang TB, Lee SR, Yang SH (2021). The Role of tumor necrosis factor alpha (TNF-α) in autoimmune disease and current tnf-α inhibitors in therapeutics. Int J Mol Sci. 22(5):2719.

29. Song L, Qiu Q, Ju F, Zheng C (2024). Mechanisms of doxorubicin-induced cardiac inflammation and fibrosis; therapeutic targets and approaches. Arch Biochem Biophys. 761:110140.

30. Mahdavi Sharif P, Jabbari P, Razi S, Keshavarz-Fathi M, Rezaei N, Rezaei N (2020). Importance of TNF-alpha and its alterations in the development of cancers. Cytokine. 130:155066.

31. de Lima Junior EA, Yamashita AS, Pimentel GD, De Sousa LG, Santos RV, Gonçalves CL, Streck EL, de Lira FS, Rosa Neto JC (2016). Doxorubicin caused severe hyperglycaemia and insulin resistance, mediated by inhibition in AMPk signalling in skeletal muscle. J Cachexia Sarcopenia Muscle. 7(5):615–625.

32. Haybar H, Goudarzi M, Mehrzadi S, Aminzadeh A, Khodayar MJ, Kalantar M, Fatemi I (2019). Effect of gemfibrozil on cardiotoxicity induced by doxorubicin in male experimental rats. Biomed Pharmacother. 109:530–535.

33. Abdulkareem Aljumaily SA, Demir M, Elbe H, Yigitturk G, Bicer Y, Altinoz E (2021). Antioxidant, anti-inflammatory, and anti-apoptotic effects of crocin against doxorubicin-induced myocardial toxicity in rats. Environ Sci Pollut Res. 28:65802–65813.

34. Chatterjea MN, Shinde R (2012). Textbook of medical biochemistry (8th ed.). Jaypee Brothers Medical Publishers, New Delhi, London; Page: 581-587.

35. Abali EE, Cline CD, Franklin DS, Viselli SM (2020). Lippincott illustrated reviews: Biochemistry (8th ed.). Wolters Kluwer, New York, Tokyo; Page: 746-770.

36. Alves de Lima E, Junior, Oliveira de Souza C, Abílio de Souza Teixeira A, Batatinha HA, de Santos Lira F, Neto JC (2014). Doxorubicin leads to impaired insulin signaling in skeletal muscle. Cancer Metab. 2(Suppl 1):P2.

37. Clemente-Suárez VJ, Redondo-Flórez L, Beltrán-Velasco AI, Martín-Rodríguez A, Martínez-Guardado I, Navarro-Jiménez E, Laborde-Cárdenas CC, Tornero-Aguilera JF (2023). The role of adipokines in health and disease. Biomedicines. 11(5):1290.

38. Ouchi N, Parker JL, Lugus JJ, Walsh K (2011). Adipokines in inflammation and metabolic disease. Nat Rev Immunol. 11(2):85–97.

39. Jiang Z, Zhao M, Voilquin L, Jung Y, Aikio MA, Sahai T, Dou FY, Roche AM, Carcamo-Orive I, Knowles JW, Wabitsch M, Appel EA, Maikawa CL, Camporez JP, Shulman GI, Tsai L, Rosen ED, Gardner CD, Spiegelman BM, Svensson KJ (2021). Isthmin-1 is an adipokine that promotes glucose uptake and improves glucose tolerance and hepatic steatosis. Cell Metab. 33(9):1836–1852.e11.

40. Shakhawat HM, Hazrat Z, Zhou Z (2022). Isthmin—a multifaceted protein family. Cells. 12(1):17.

41. Lei X, Chen H, Xu Y, Yang Z, Zhang L, Wang C, Du H (2024). Serum isthmin-1 is a potential biomarker for metabolic dysfunction associated fatty liver disease in patients with metabolic syndrome and type 2 diabetes mellitus. BMJ Open Diabetes Res Care. 12(5):e004514.

42. Menghuan L, Yang Y, Qianhe M, Na Z, Shicheng C, Bo C, XueJie YI (2023). Advances in research of biological functions of isthmin-1. J Cell Commun Signal. 17(3):507–521

43. Bürgi W, Schmid K (1961). Preparation and properties of zin-α2-glycoprotein of normal human plasma. J Biol Chem. 236(4):1066–1074.

44. Shigefuku R, Iwasa M, Eguchi A, Tempaku M, Tamai Y, Fujiwara N, Sugimoto R, Tanaka H, Sugimoto K, Kobayashi Y, Nakagawa H (2024). Serum zinc-α2-glycoprotein levels are associated with the hepatorenal function and predict the survival in cases of chronic liver disease. Intern Med (Tokyo). 63(1):31–41.

45. Prakash U, Bharathidevi SR, Nadig RR, Raman R, Rao GS, Bhende M (2023). Zinc alpha 2 glycoprotein (ZAG): apotential novel pharmacological target in diabetic retinopathy.

46. Vuong QV, Bowyer MC, Roach PD (2011). L-Theanine: properties, synthesis and isolation from tea. J Sci Food Agric. 91(11):1931–1939.

47. Fiori J, Pasquini B, Caprini C, Orlandini S, Furlanetto S, Gotti R (2018). Chiral analysis of theanine and catechin in characterization of green tea by cyclodextrin-modified micellar electrokinetic chromatography and high performance liquid chromatography. J Chromatogr A. 1562:115–122.

48. Zhongying L, Qiansong R, Ke P, Qin L, Ting Y, Yuqiao D, Shimao F, Wenjia Z (2022). Flavor characteristics of three amino acid monomers based on electronic tongue. Food Sci Technol. 47:296–302.

49. Lin L, Zeng L, Liu A, Peng Y, Yuan D, Zhang S, Li Y, Chen J, Xiao W, Gong Z (2020). L-theanine regulates glucose, lipid, and protein metabolism via insulin and AMP-activated protein kinase signaling pathways. Food Funct. 11(2):1798–1809.

50. Xu W, Kong Y, Zhang T, Gong Z, Xiao W (2023). L-theanine regulates lipid metabolism by modulating gut microbiota and bile acid metabolism. J Sci Food Agric. 103(3):1283–1293.

51. Kurihara S, Shibahara S, Arisaka H, Akiyama Y (2007). Enhancement of antigen-specific immunoglobulin G production in mice by co-administration of L-cystine and L-theanine. J Vet Med Sci. 69(12):1263–127052.

52. Zhao S, Cao W, Xing S, Li L, He Y, Hao Z, Wang S, He H, Li C, Zhao Q, Gao D (2019). Enhancing effects of theanine liposomes as chemotherapeutic agents for tumor therapy. ACS Biomater Sci Eng. 5(7):3373–3379.

53. Saeed M, Yatao X, Hassan F-U, Arain MA, Abd El-Hack ME, Noreldin AE, Sun C (2018). Influence of graded levels of L-theanine dietary supplementation on growth performance, carcass traits, meat quality, organs histomorphometry, blood chemistry and immune response of broiler chickens. Int J Mol Sci. 19(2):462.

54. Pérez-Vargas JE, Zarco N, Vergara P, Shibayama M, Segovia J, Tsutsumi V, Muriel P (2016). L-theanine prevents carbon tetrachloride-induced liver fibrosis via inhibition of nuclear factor κB and down-regulation of transforming growth factor β and connective tissue growth factor. Hum Exp Toxicol. 35(2):135–146.

55. Zeng L, Lin L, Chen L, Xiao W, Gong Z (2021). L-theanine ameliorates D-galactose-induced brain damage in rats via inhibiting AGE formation and regulating Sirtuin1 and BDNF signaling pathways. Oxid Med Cell Longev. 2021:8850112.

56. Lyu W, Ouyang M, Ma X, Han T, Pi D, Qiu S (2021). Kai-Xin-San attenuates doxorubicin-induced cognitive impairment by reducing inflammation, oxidative

stress, and neural degeneration in 4T1 breast cancer mice. Evid Based Complement Alternat Med. 2021:5521739.

57. Uchiyama M, Mihara M (1978). Determination of malonaldehyde precursor in tissues by thiobarbituric acid test. Anal Biochem. 86(1):271–278.

58. Avagimyan A, Pogosova N, Rizzo M, Sarrafzadegan N (2025). Doxorubicin-induced cardiometabolic disturbances: what can we do? Front Clin Diabetes Healthc. 6:1537699.

59. Heart EA, Karandrea S, Liang X, Balke ME, Beringer PA, Bobczynski EM, Zayas-Bazán Burgos D, Richardson T, Gray JP (2016). Mechanisms of doxorubicin toxicity in pancreatic β-Cells. Toxicol Sci. 152(2):395–405.

60. Li MJ, Sun WS, Yuan Y, Zhang YK, Lu Q, Gao YZ, Ye T, Xing DM (2022). Breviscapine remodels myocardial glucose and lipid metabolism by regulating serotonin to alleviate doxorubicin-induced cardiotoxicity. Front Pharmacol. 13:930835.

61. Belger C, Abrahams C, Imamdin A, Lecour S (2023). Doxorubicin-induced cardiotoxicity and risk factors. Int J Cardiol Heart Vasc. 50:101332.

62. Jahdkaran M, Sistanizad M (2025). From lipids to glucose: investigating the role of dyslipidemia in the risk of insulin resistance. J Steroid Biochem Mol Biol. 250:106744.

63. Wu, Y. Z., Wang, K. X., Ma, X. D., Wang, C. C., Chen, N. N., Xiong, C., Li, J. X., & Su, S. W. (2023). Therapeutic effects of atorvastatin on doxorubicin-induced hepatotoxicity in rats via antioxidative damage, anti-inflammatory, and anti-lipotoxicity. Journal of biochemical and molecular toxicology, 37(6), e23329.

64. Purnamasidhi CAW, Suega K, Bakta IM (2019). Association between lactate dehydrogenase levels and chemotherapy response in elderly patients with Non-Hodgkin Lymphoma. Open Access Maced J Med Sci. 7(12):1984–1986.

65. Ma J, Li P, An L, Zhang T, Li G (2022). Chemoprotective effect of theanine in 1,2-dimethylhydrazine-induced colorectal cancer in rats via suppression of inflammatory parameters. J Food Biochem. 46(2):e14073.

66. Sawicki KT, De Jesus A, Ardehali H (2023). Iron metabolism in cardiovascular disease: physiology, mechanisms, and therapeutic targets. Circ Res. 132(3):379–396.

67. Kural BV, Mohamed SA, Kör S, Malkoç MA, Yuluğ E, Tekmeh HH, Örem A (2023). Caution may be required in using L-theanine in diabetes mellitus: A study on the rats. Biochem Biophys Res Commun. 666:170–178.

68. Ma C, Xu A, Zuo L, et al. (2025). Methionine dependency and restriction in cancer: exploring the pathogenic function and therapeutic potential. pharmaceuticals (Basel). 18(5):640.

69. Xin Y, Zhang Y, Yuan Z, Li S (2025). Methionine is an essential amino acid in doxorubicin-induced cardiotoxicity through modulating mitophagy. Free Radic Biol Med. 232:28–39.

70. Fan R, Wang Y, Zhang J, An X, Liu S, Bai J, Li J, Lin Q, Xie Y, Liao J, Xia Y (2023). Hyperhomocysteinaemia promotes doxorubicin-induced cardiotoxicity in mice. Pharmaceuticals (Basel).

71. Mirzaei S, Zarrabi A, Hashemi F, Zabolian A, Saleki H, Azami N, Hamzehlou S, Farahani MV, Hushmandi K, Ashrafizadeh M, Khan H, Kumar AP (2021). Nrf2 signaling pathway in chemoprotection and doxorubicin resistance: potential application in drug discovery. Antioxidants. 10(3):349.

72. Zhao X, Tian Z, Sun M, Dong D (2023). Nrf2: a dark horse in doxorubicin-induced cardiotoxicity. Cell Death Discov. 9(1):261.

73. Shen J, Chen S, Li X, Wu L, Mao X, Jiang J, Zhu D (2024). Salidroside mediated the Nrf2/GPX4 pathway to attenuates ferroptosis in parkinson's disease. Neurochem Res. 49(5):1291–1305.

74. Arıkan Malkoç M, Özer Yaman S, Yuluğ E, Işık S, Kural B (2025). L-theanine ameliorates doxorubicin-induced ovarian toxicity by reducing endoplasmic reticulum stress. Food Sci Nutr. 13(4):e70150.

75. Altınkaynak Y, Kural B, Akcan BA, Bodur A, Özer S, Yuluğ E, Munğan S, Kaya C, Örem A (2018). Protective effects of L-theanine against doxorubicin-induced nephrotoxicity in rats. Biomed Pharmacother. 108:1524–1534.

76. Renu K, VG A, PB TP, Arunachalam S (2018). Molecular mechanism of doxorubicin-induced cardiomyopathy – an update. Eur J Pharmacol. 818:241–253.

77. Yang CC, Wang MH, Soung HS, Tseng HC, Lin FH, Chang KC, Tsai CC (2023). Through its powerful antioxidative properties, L-theanine ameliorates vincristine-induced neuropathy in rats. Antioxidants. 12(4):803.

78. Olechnowicz J, Tinkov A, Skalny A, Suliburska J (2018). Zinc status is associated with inflammation, oxidative stress, lipid, and glucose metabolism. J Physiol Sci. 68(1):19–31.

APPENDICES

CURRICULUM VITAE

PERSONEL INFORMATIONS

Name Surname	**:** Entesar Ali Ahmed AMER
Nationality	**:** Yemen
Birth Date	**:**
Phone Number (Business)	**:**
E-mail	**:**
Correspondence Address	**:**
(Business)	

EDUCATION INFORMATION

Degree	Name of the School	Graduation Year
BSc	Department of Biochemistry, Faculty of Science / King Abdul Aziz University, Jeddah, KSA	2015
High School	4th Girls High School, Jeddah, KSA	2010

LANGUAGES

1. Arabic
2. English
3. Turkish

REWARDS / INCENTIVES SCHOLARSHIPS

1. Full funded scholarship for studying Master's degree by YTB (Presidency for Turks Abroad and Related Communities)
2. Graduated with (First Honor) from biocemistry deparment, faculty of science

HOBBIES

1. Chorechet
2. Arabic calligraphy